Arteriosclerosis, Thrombosis, and Vascular Biology

BASIC SCIENCES

Expression of CD70 Modulates Nitric Oxide and Redox Status in Endothelial Cells

Arvind K. Pandey, Markus Waldeck-Weiermair, Quinn S. Wells, Wusheng Xiao, Shambhu Yadav, Emrah Eroglu, Thomas Michel, Joseph Loscalzo

BACKGROUND: Endothelial dysfunction is a critical component in the pathogenesis of cardiovascular diseases and is closely associated with nitric oxide (NO) levels and oxidative stress. Here, we report on novel findings linking endothelial expression of CD70 (also known as CD27 ligand) with alterations in NO and reactive oxygen species.

METHODS: CD70 expression was genetically manipulated in human aortic and pulmonary artery endothelial cells. Intracellular NO and hydrogen peroxide (H_2O_2) were measured using genetically encoded biosensors, and cellular phenotypes were assessed.

RESULTS: An unbiased phenome-wide association study demonstrated that polymorphisms in CD70 associate with vascular phenotypes. Endothelial cells treated with CD70-directed short-interfering RNA demonstrated impaired wound closure, decreased agonist-stimulated NO levels, and reduced eNOS (endothelial nitric oxide synthase) protein. These changes were accompanied by reduced NO bioactivity, increased 3-nitrotyrosine levels, and a decrease in the eNOS binding partner heat shock protein 90. Following treatment with the thioredoxin inhibitor auranofin or with agonist histamine, intracellular H_2O_2 levels increased up to 80% in the cytosol, plasmalemmal caveolae, and mitochondria. There was increased expression of NADPH oxidase 1 complex and gp91phox; expression of copper/zinc and manganese superoxide dismutases was also elevated. CD70 knockdown reduced levels of the H_2O_2 scavenger catalase; by contrast, glutathione peroxidase 1 expression and activity were increased. CD70 overexpression enhanced endothelial wound closure, increased NO levels, and attenuated the reduction in eNOS mRNA induced by TNFα.

CONCLUSIONS: Taken together, these data establish CD70 as a novel regulatory protein in endothelial NO and reactive oxygen species homeostasis, with implications for human vascular disease.

GRAPHIC ABSTRACT: A graphic abstract is available for this article.

Key Words: CD27 ligand ■ endothelial dysfunction ■ homeostasis ■ nitric oxide synthase type III ■ reactive oxygen species

Vascular dysfunction is a hallmark of a wide array of cardiovascular diseases. Endothelial cells (ECs) are a key upstream target of these disease states, with dysregulation of ECs often serving as an initiating step in the pathogenesis of vascular dysfunction. A cardinal finding of endothelial injury is a reduction in bioactive nitric oxide (NO), which plays a central role in maintaining endothelial and vasomotor homeostasis.[1] Dysregulation of eNOS (endothelial nitric oxide synthase, also known as nitric oxide synthase III), the primary source of vascular NO, can have far-reaching effects on endothelial function and homeostasis. Impairment in eNOS is closely associated with alterations in cellular redox balance, which can broadly promote oxidative injury and further dysfunction in the cardiovascular system.[2] A number of inflammatory signals, generated in response to local injury or immune-mediated processes, can induce these effects in the endothelium, although an understanding of this inflammatory/

Correspondence to: Joseph Loscalzo, MD, PhD, Department of Medicine, Brigham and Women's Hospital and Harvard Medical School, 75 Francis St, Boston, MA 02115. Email jloscalzo@rics.bwh.harvard.edu

Supplemental Material is available at https://www.ahajournals.org/doi/suppl/10.1161/ATVBAHA.122.317866.

For Sources of Funding and Disclosures, see page 1183.

Nonstandard Abbreviations and Acronyms

eNOS	endothelial nitric oxide synthase
HAEC	human aortic endothelial cell
HPAEC	human pulmonary artery endothelial cell
NO	nitric oxide
PheWAS	phenome-wide association study
ROS	reactive oxygen species
siRNA	short-interfering RNA
SOD	superoxide dismutase
TNF	tumor necrosis factor

immune-endothelial link at baseline and in disease states remains incomplete.

The TNF (tumor necrosis factor) superfamily (TNFSF) of ligands is a large and diverse family of transmembrane proteins typically active on the cell surface or in the extracellular space following proteolytic cleavage. TNFSF members have wide-ranging roles and mediate an array of inflammatory and immunologic functions, typically through interaction with their respective receptors, which are members of the TNF receptor superfamily. There is increasing recognition of the role of TNFSF ligands in vascular disease. The most well-characterized of these is TNF-α (TNF-alpha), which is known to induce endothelial dysfunction by enhancing the production of reactive oxygen species (ROS) and reducing eNOS-derived bioactive NO.[3] Similarly, other TNFSF members have been linked to vascular disease phenotypes ranging from atherosclerosis to pulmonary hypertension, including CD137 ligand, OX40 ligand, and CD40 ligand.[4–13] TNF-α, CD40 ligand, and OX40 ligand have all been shown to be expressed by endothelial cells, although the functional consequences of these endothelial-expressed TNSFs has been investigated primarily in the context of autocrine and paracrine signaling through their respective receptors on endothelial cells.[7,14,15] Whether or not TNFSF expression may have a more fundamental role in endothelial biology independent of receptor-mediated signaling has not been well-defined.

CD70, also known as CD27 ligand, is a TNFSF member that primarily has been characterized in professional antigen-presenting cells, including dendritic cells, macrophages, and B cells. CD70 expression is highly regulated, with relatively low baseline expression in these cells and increased expression in response to antigen-presenting cell stimulation.[16] CD70 serves as the ligand for the TNF receptor superfamily member CD27. Through the interaction of CD70 on antigen-presenting cells and CD27 on T and B cells, the CD27-CD70 axis promotes several effector responses, including priming, effector maturation, and polarization of T cell subtypes;

Highlights

- CD70 is a novel regulator of endothelial function and homeostasis.
- Loss of CD70 is associated with decreased expression of endothelial nitric oxide synthase, leading to reduced nitric oxide bioavailability and bioactivity.
- Reactive oxygen species in the form of hydrogen peroxide are increased in the absence of CD70 expression.

for example, the CD27-CD70 axis is important for the formation of T effector memory (T_{EM}) cells.[16] In mice, CD70 expression on macrophages and dendritic cells is increased in response to hypertensive stimuli, and global CD70 knockdown can reduce T_{EM} accumulation in the kidney and abrogate elevations in blood pressure after exposure to repeated hypertensive stimuli.[17] More recently, CD70 expression has been recognized on a number of solid tumor cancer cells, where it may function to promote immune evasion of tumor cells, and it is being investigated as a target for novel cancer immunotherapies.[18–23] CD70 expression has been reported in tumor microenvironments, including on endothelial cells,[19] as well as in inflammatory vascular wall lesions of carotid arteries in patients with Takayasu's arteritis.[24] The functional consequences of this vascular expression of CD70, both in pathological scenarios and in the normal vasculature, are not known. One recent study showed that $CD70^{-/-}$ mice have reduced collateral arteries and decreased angiogenesis following hindlimb ischemia.[25] However, further characterization of this TNFSF member has been exceedingly limited in the vascular context. In this study, we have identified a novel role for CD70 in endothelial cells.

METHODS

The data that support the findings of this study are available from the corresponding author upon reasonable request.

Cell Culture

Primary human aortic endothelial cells (HAECs) and pulmonary artery endothelial cells (HPAECs) were purchased from Lonza (Walkersville, MD) and grown in EBM-2 media with EGM-2 supplements (Lonza) but without an antimicrobial additive. Cells were grown at 37 °C with 5% CO_2 and 95% humidity; cell media was changed every other day, and cells from passage 3 to passage 9 were utilized for all experiments. TNF-α was purchased from R&D Biosystems (Minneapolis, MN), and HAECs and HPAECs were treated at a concentration of 50 ng/mL for 0.5 to 48 hours. Glucose-free medium was purchased from Cell Biologics (Chicago, IL) and HPAECs were grown in this medium overnight. For hypoxia treatment, HPAECs were placed in a modular

incubator chamber (Billups-Rothenberg, San Diego, CA) flushed with 100 L of a gas mixture containing 0.2% O_2, 5% CO_2, and balanced with N2 (Airgas) then incubated at 37°C overnight.

siRNA Treatment

OnTARGETplus short-interfering RNA (siRNA) smart pool was purchased from Dharmacon (Lafayette, CO) to target human *CD70* (L009952-00-0005; siCD70). OnTARGETplus nontargeting scrambled control siRNA (D-001810-10-05; siCtrl) was purchased and utilized for control experiments. Cells were transfected with siRNA using Lipofectamine RNAiMAX transfection reagent (Life Technologies, Carlsbad, CA) according to the manufacturer's protocols. Following overnight transfection, media was changed daily, and analyses were performed 2 to 4 days post-transfection.

Western Blot

Cells were lysed in ice-cold RIPA or NP-40 lysis buffer, supplemented with a protease and phosphatase inhibitor cocktail (ThermoFisher Scientific, Waltham, MA), and protein was isolated. Protein quantification was performed with a detergent-compatible Lowry assay (Bio-Rad, Hercules, CA). Samples (10–30 µg of protein) were separated on SDS-PAGE and then transferred to a polyvinylidene fluoride membrane using the Trans-Blot Turbo system (Bio-Rad). The membrane was blocked with 5% nonfat dry milk and probed with primary antibodies diluted in blocking solution. The following primary antibodies were utilized at the indicated stock dilution and final working concentration: 3-nitrotyrosine (Cell Signaling Technology, 9691, 1:1000, 0.018 µg/mL), catalase (Athens Research and Technology, 01-05-030000, 1:1000, 1.96 µg/mL), caveolin-1 (Cell Signaling Technology, 3267, 1:4000, 0.17 µg/mL), CD70 (R&D System, AF-2738, 1:500, 0.5 µg/mL), eNOS (Cell Signaling Technology, 32027, 1:500, 0.05 µg/mL), gp91phox (Santa Cruz Biotechnology, sc-130543, 1:1000, 0.2 µg/mL), GPx (glutathione peroxidase) 1 (MBL International, M015-3, 1:1000, 1 µg/mL), Hsp90 (heat shock protein 90; Cell Signaling Technology, 4877, 1:1000, 1.3 µg/mL), mCherry (Cell Signaling Technology, 43590, 1:1000, 0.2 µg/mL) NOX (NADPH oxidase) 1 (Proteintech, 17772-1-AP, 1:1000, 0.4 µg/mL), SOD1 (Cell Signaling Technology, 4266, 1:1000, 1.1 µg/mL), SOD2 (Cell Signaling Technology, 13141, 1:1000, 0.049 µg/mL). After washing, membranes were probed with anti-mouse (Cell Signaling Technology, 7076, 1:2000, 0.092 µg/mL), anti-rabbit (Cell Signaling Technology, 7074, 1:2000, 0.03 µg/mL), or anti-goat (Abcam, ab205723, 1:4000, 0.5 µg/mL) secondary antibody and then developed using the WesternBright enhanced chemiluminescence kit according to the manufacturer's protocols (Advansta, San Jose, CA). Blots were imaged using a Bio-Rad ChemiDoc system.

Glutathione Peroxidase Activity

HAECs and HPAECs were treated with control or CD70-directed siRNA for 4 days, and cells were then harvested for assessing GPx activity using an enzyme activity assay kit according to the manufacturer's protocol (Cayman Chemical, Ann Arbor, MI).

Cyclic GMP Assay

HAECs and HPAECs were transfected with siCtrl or siCD70; 4 days after transfection, cells were treated with 0.3 M of 3-isobutyl-1-methylxanthine for 30 minutes. Cells were then stimulated with 30 µM ATP (ATP) for 10 minutes and subsequently lysed with 0.1 N HCl. Cell lysis supernatants were isolated and total intracellular cGMP (cyclic guanosine monophosphate) levels were determined using an ELISA kit according to the manufacturer's protocols (Enzo Life Sciences, Farmingdale, NY).

Nitrite/Nitrate Assay

HPAECs were transfected with siCtrl or siCD70, and 4 days after transfection, media was changed to basal EBM media (Lonza) with 2.5% fetal bovine serum with no other added supplements for 4 hours. Following this period, cell supernatants were collected and assayed for total nitrite/nitrate content using a commercially available kit according to the manufacturer's protocol (Cayman Chemical). Cells were harvested to determine protein content for normalization.

Quantitative Real-Time PCR

Total RNA was isolated using RNeasy miniprep kit (Qiagen, Germantown, MA) according to the manufacturer's protocols. RNA concentration and quality were assessed using a NanoDrop One system (ThermoFisher Scientific). RNA (1–4 µg) was utilized for reverse transcription into cDNA using the High Capacity cDNA Reverse Transcription kit (Applied Biosystems, Foster City, CA), after which cDNA dilutions were used to amplify gene targets using the TaqMan Universal PCR kit (ThermoFisher Scientific) on a 7900HT Fast Realtime PCR machine using commercially available primers (ThermoFisher; Table S1). Expression of targets was calculated using the $2^{-\Delta\Delta Ct}$ method and normalized to β-actin transcript. For gp91phox transcript analysis, custom primers were utilized (forward: 5'-TGGAGAGCCAGATGCAGGAA-3', reverse: 5'-TCCTCATCATGGTGCACAGC-3'), and data were normalized to RNA polymerase II subunit A transcript (forward: 5'-TCCAGAGCGAGTGCATGAGA-3', reverse: 5'-CAATCATCCACTCTGGCCGT-3').

Phenome Wide Association Study

To assess for associations between genetic variation in CD70 and human disease phenotypes, we utilized BioVU, the Vanderbilt University biobank that links de-identified electronic health records to DNA samples and genotype data.[26] Analyses were conducted in a cohort of 12 834 adults of European ancestry previously genotyped on the Illumina Multi-Ethnic Genotyping Array (MEGAEX). Quality control analyses used PLINK v 1.90β3[27] and included reconciling strand flips, verifying that allele frequencies were concordant among data sets, and identifying duplicate and related individuals.[28] Data sets were standardized using the HRC-1000G-check tool v4.2.5 (http://www.well.ox.ac.uk/~wrayner/tools/) and prephased using SHAPEIT.[29]

The PheWAS (Phenome Wide Association Study) method leverages a validated, curated medical phenome that hierarchically groups the International Classification of Disease billing codes into phenotypes ("PheWAS codes") (https://phewas.mc.vanderbilt.edu/), each with defined control groups.[30,31]

Association testing utilized logistic regression adjusted for age and sex. Analyses were restricted to those phenotypes with ≥200 cases (N=534). To adjust for multiple testing, we employed a Bonferroni adjustment, with a $P<9.4\times10^{-5}$ considered statistically significant (0.05/534 phenotypes). A gene map was constructed using the online University of California Santa Cruz Genome Browser (http://genome.ucsc.edu) with the GRCh38/hg38 assembly.[32,33]

Endothelial Monolayer Wound Healing Assay

Endothelial monolayer wound healing in response to a scratch was assessed as previously described.[34] Briefly, HPAECs were grown to confluence in 6-well plates. At time point 0 hour, the cell monolayer was scratched using a sterile P200 pipet tip to create a cell-free area running the length of the well. Images were obtained at time points 0 and 6 hours post-scratch using a Nikon TE2000-S microscope. The cell-free area was measured using ImageJ software and the percent recovery after 6 hours was calculated using the formula (area at 0 h—area at 6 h)/(area at 0 h) * 100.

Real-Time NO, Calcium, and Hydrogen Peroxide Imaging

The genetically encoded biosensor cyan geNOp (c-geNOp) was utilized for real-time, single-cell imaging of NO in HAECs and HPAECs as described previously.[35–37] Briefly, c-geNOp is a genetically encoded fluorescence biosensor containing the NO-binding GAF domain derived from the prokaryotic NorR protein linked to a cyan fluorescent protein. HAECs and HPAECs were grown on No. 1.5 30 mm glass coverslips (Bioptechs, Butler, PA) and treated with control or CD70-directed siRNA. For NO imaging, 3 days post-transfection, cells were treated with adenoviral vector expressing the c-geNOp probe at a multiplicity of infection of 15 (indicating ≈ 4 million virus particles per treatment). After overnight incubation, cells were washed with PBS and then incubated in a HEPES physiological salt solution (140 mmol/L NaCl, 5 mmol/L KCl, 2 mmol/L $CaCl_2$, 1 mmol/L $MgCl_2$, 10 mmol/L D-glucose and 1 mmol/L HEPES, pH 7.4) supplemented with 1 mmol/L iron(II) fumarate and 1 mmol/L L-ascorbic acid for 20 minutes at 37 °C. Following this incubation, cells were transferred into an imaging buffer (138 mmol/L NaCl, 5 mmol/L KCl, 2 mmol/L $CaCl_2$, 1 mmol/L $MgCl_2$, 1 mmol/L HEPES, 2.6 mmol/L $NaHCO_3$, 0.44 mmol/L KH_2PO_4, 0.34 mmol/L Na_2HPO_4, 10 mmol/L D-glucose, 0.1% vitamins, 0.2% essential amino acids and 1% penicillin/streptomycin, pH 7.4) for 2 hours. Coverslips were mounted on a custom live-cell imaging platform that allowed for stable superfusion of physiological salt solution with or without agonist. The c-geNOp probe was imaged in real time using an excitation wavelength of 420 nm; emission was recorded at 480 nm. Images were captured using a CCD camera (Hamamatsu, Bridgewater, NJ) and Metafluor Software (Molecular Devices, San Jose, CA) every 3 seconds. After baseline measurements, cells were exposed to 30 μM ATP through the superfusate for 120 seconds to achieve maximal NO response, followed by a washout period of at least 3 minutes. Following recordings, background readings were subtracted from single-cell NO measurements. Change in NO signal from the intensiometric c-geNOp was calculated using the formula, $\Delta F=1-(F/F_0)\times100$, where F_0 is the magnitude of baseline NO signal intensity. Maximum cellular NO level was determined for each treatment group in response to ATP treatment.

For cells undergoing real-time calcium imaging, Fura-2 AM (ThermoFisher Scientific) was diluted to 3.3 μM in imaging buffer. Cells were washed and incubated in this solution for 40 minutes. Cells were then washed again and placed in imaging buffer for 2 hours before imaging. Following this incubation, cells were excited at both 340 and 380 nm, and emission was analyzed at 520 nm every 3 seconds. After baseline measurements, cells were stimulated with 30 μM ATP through the superfusate for 90 seconds. Background readings were subtracted and maximum intracellular Ca^{2+} flux was calculated by determining the normalized ratio, R/R_0, where R is the ratio of the 340 nm to the 380 nm signals, and R_0 is the baseline 340/380 ratio.

For intracellular H_2O_2 imaging, the novel genetic biosensor Hyper7.2 was utilized.[38] In brief, Hyper7.2 is a ratiometric, genetically encoded biosensor composed of an OxyR regulatory domain derived from *Neisseria meningitidis* for sensing H_2O_2 integrated with a circularly permuted yellow fluorescent protein. HAECs and HPAECs after 3 days of siRNA treatment were subsequently transfected with a plasmid expressing either cytosolic-directed Hyper7.2, caveolin-targeted Hyper7.2, or mitochondrial-targeted Hyper7.2 using Lipofectamine 3000 (Life Technologies). The manufacturer's protocol was modified by performing transfection for 6 to 12 hours in regular media followed by replacement with fresh media. The next day, cells were placed in phenol-free EBM (Lonza) without supplements or serum for 1 hour and then imaged as previously described.[38] Briefly, cells were excited at both 420 and 490 nm, and emissions were recorded at 520 nm every 10 seconds. After baseline measurements, cells were stimulated with 1 μM auranofin or 30 μM histamine through the superfusate for 10 to 15 minutes. Background readings were subtracted and intracellular H_2O_2 was calculated by determining the ratio, R/R_0, where R is the ratio of the 490 nm to the 420 nm signals, and R_0 is the baseline 490/420 ratio. Data were analyzed using a 2-tailed Mann-Whitney *U* test as the differing distributions between control and CD70-knockdown groups precluded an assumption of normality across all samples.

Superoxide Determination

HPAECs were grown on No. 1.5 30 mm coverslips and treated with control versus CD70-directed siRNA. Four days post-transfection, cells were loaded with 10 μM dihydroethidium (DHE) (ThermoFisher) diluted in complete cell medium for 60 minutes. Following loading, cells were washed with PBS and then imaged in real-time using an excitation wavelength of 488 nm with emission detected at 588 nm every 5 seconds for baseline measurements. Following basal assessment of fluorescence, cells were stimulated with 30 μM menadione through the superfusate for 5 minutes, followed by treatment with 30 μM menadione plus 100 U/mL pegylated SOD (superoxide dismutase; Sigma-Aldrich, St. Louis, MO). The SOD-inhibitable component of the menadione-stimulated signal was assessed to be more specific for 2-hydroxyethidium, the superoxide-derived fluorescence product of DHE.

CD70 Overexpression

We constructed a plasmid to overexpress CD70 linked to the fluorescent protein mCherry. The coding sequence of

CD70 was amplified from HUVEC cDNA by PCR using a Q5 High-Fidelity DNA Polymerase (New England Biolabs Inc., NEB, Ipswich, MA) with gene specific primers including recognition sites for NheI and *Eco*RI as follows: forward 5'-AAAGCTAGCATGCCGGAGGAGGGTTCGGG-3' and reverse 5'-AAAGAATTCGGGGCGCACCCACTGCACTCC-3'. The PCR product was digested with indicated restriction enzymes (NEB) and N-terminally fused to a mCherry-myc-HIS tag into a pcDNA3.1(-) vector using the Quick Ligation Kit (NEB). HPAECs were transfected with this construct versus a control plasmid of the same vector backbone using Lipofectamine 3000. The manufacturer's protocol was modified by performing transfection overnight in regular media followed by replacement with fresh media.

Statistical Analysis

All statistics were performed, and graphs generated in Prism 9 (GraphPad, San Diego, CA) or in Microsoft Excel (Redmond, WA). All standard bar, scatter, and dot plots have summary data with errors bars representing mean±SE; violin plots contain lines for the median and quartiles of the distribution. To determine statistical significance for differences in observations in experiments with $n<6$, a nonparametric Mann-Whitney *U* test was utilized. For $n\geq6$, normality was assessed with the Shapiro-Wilk test using $\alpha=0.05$, and the assumption of equal variances was analyzed using an *F*-test. For all groups that passed these tests, a Student *t* test was utilized. For those that did not pass either of the 2 tests, a nonparametric Mann-Whitney *U* test was utilized to determine significance. All replicates performed represent at least 4 independent biological experiments.

Major Resources Supplement

Please see the Major Resources Table in the Supplemental Material.

RESULTS

CD70 Polymorphisms Correlate With Human Vascular Disease Phenotypes

To investigate whether CD70 influences cardiovascular phenotypes, we performed a PheWAS to elucidate the relationships between SNPs (single nucleotide polymorphisms) and human disease phenotypes. In an unbiased phenome-wide analysis, we identified a statistically significant association (corrected for multiple comparisons) between the SNP rs11458827 (representing an insertion of thymine compared with the reference genome sequence in the intronic sequence between exons 2 and 3 of the *CD70* gene) and the phenotype, "peripheral vascular disease, unspecified" (odds ratio: 0.8 [95% CI, 0.70–0.91]; $P=7.65\times10^{-5}$; Figure 1A). This SNP is located in a DNase hypersensitivity domain and is associated with histone H3 marks, which are typical of regulatory elements (Figure 1B). In secondary analyses restricted to phenotypes grouped under the "circulatory system," we found nominal associations ($P<0.05$) between rs11458827 and other cardiovascular phenotypes including "atherosclerosis" (odds ratio: 0.8 [95% CI, 0.79–0.96]; $P=1.7\times10^{-3}$), "peripheral vascular disease" (odds ratio: 0.86 [95% CI, 0.76–0.96]; $P=3.3\times10^{-3}$), and "atherosclerosis of the extremities" (odds ratio: 0.85 [95% CI, 0.72–0.98]; $P=1.5\times10^{-2}$). These data provided intriguing evidence that CD70 has a link to human cardiovascular disease from a population perspective.

CD70 Knockdown in Endothelial Cells Impairs eNOS Expression and Function

To gain mechanistic insights into how CD70 may be influencing vascular phenotypes, we investigated the consequences of CD70 knockdown on endothelial cells. Both HAECs and HPAECs were utilized to gain a broader understanding of CD70 function in different vascular beds. At baseline, endogenous expression of CD70 is readily detectable by quantitative RT-PCR. Since expression of other TNFSFs can be induced by TNF-α in endothelial cells,[39] we sought to determine if CD70 follows a similar pattern. Indeed, CD70 expression could be augmented by treatment with TNF-α, with mRNA levels increasing over 24 hours by up to 75-fold (Figure S1A and S1B); CD70 protein levels were detectable by Western blot after 48 hours of TNF-α treatment compared with vehicle control treatment (Figure S1C). We also examined the expression of CD70 in the setting of other pathological stimuli, namely hypoxia and glucose deprivation, for 24 hours. Hypoxia did not alter CD70 expression, while glucose deprivation increased CD70 mRNA; the combination of both led to a greater increase in CD70 mRNA levels (Figure S1D). Using siRNA directed against the CD70 transcript, mRNA expression was suppressed by >90% compared with control siRNA-transfected cells for up to 4 days post-transfection (Figure S1E and S1F). Suppression of CD70 had a demonstrable effect on endothelial growth, with population doubling time increased by ≈ 25% (Figure S1G). CD70 knockdown also led to a significant decrease in endothelial monolayer wound closure, indicating an impairment in endothelial migratory capacity (Figure 1C and 1D).

Since NO has a central role in maintaining endothelial homeostasis and is an early target in the pathogenesis of a number of cardiovascular diseases,[40,41] we next examined the effect of CD70 knockdown on NO levels. We measured real-time agonist-stimulated generation of NO using the genetically encoded biosensor c-geNOp, a highly specific NO probe that has been well-validated for NO measurements.[35–37] HAECs and HPAECs transfected with control and CD70-targeted siRNA were treated with adenovirus expressing c-geNOp. Following agonist stimulation of cells with ATP, individual cell fluorescence intensity was monitored in real time to deduce NO levels. Compared with control-siRNA-treated cells,

A

Phenotype	p value for association with SNP rs11458827
Peripheral vascular disease, unspecified	7.65×10^{-5}*
Atherosclerosis	1.7×10^{-3}
Peripheral vascular disease	3.3×10^{-3}
Atherosclerosis of the extremities	1.5×10^{-2}

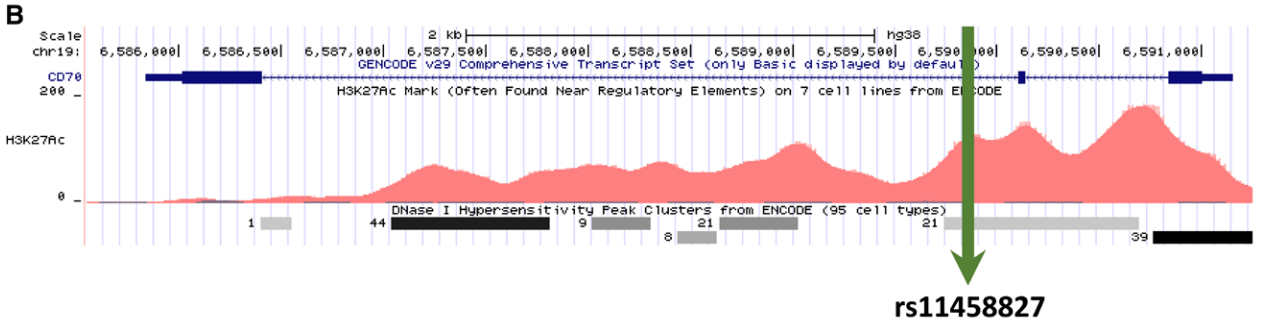

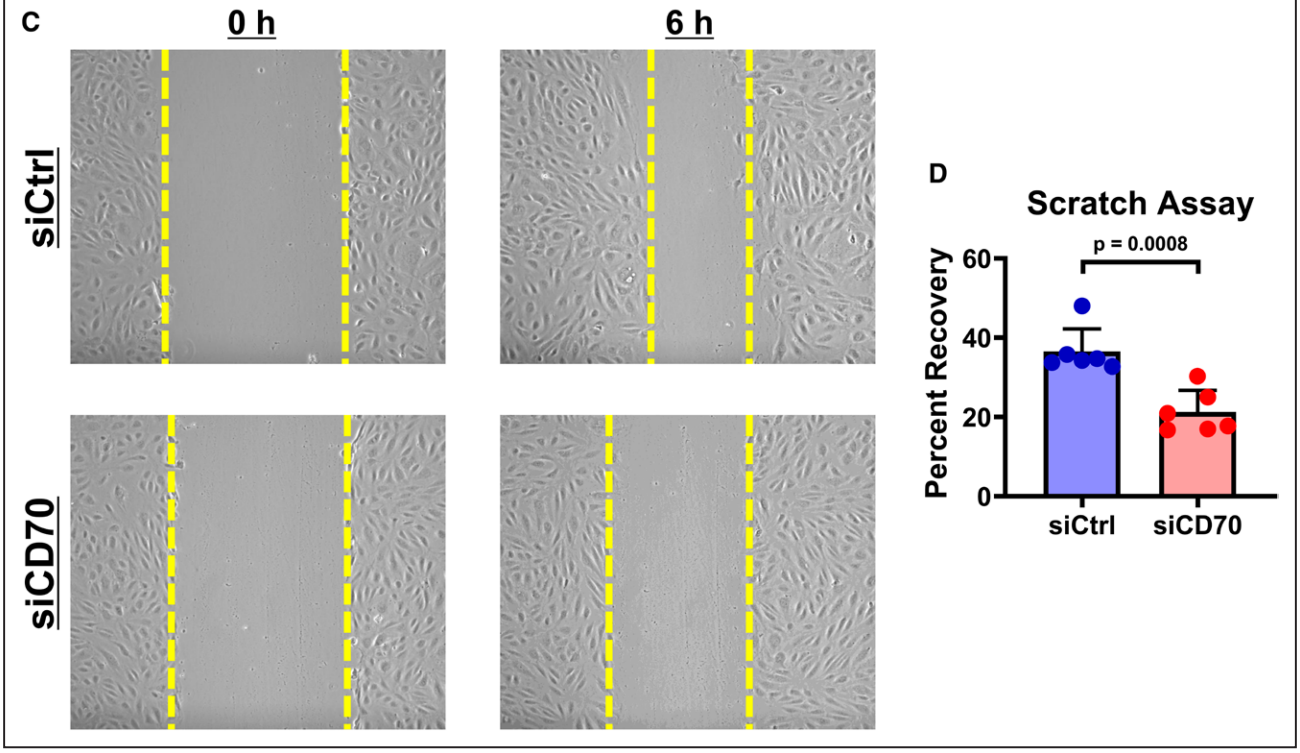

Figure 1. The CD70 SNP (single nucleotide polymorphism) associates with vascular disease in PheWAS (Phenome-Wide Association Study) and loss of CD70 impairs endothelial wound recovery.
Using an unbiased phenome-wide analysis of SNPs of CD70, rs11458827 showed a significant association with vascular disease phenotypes in humans (*$P<9.4\times10^{-5}$ corrected for multiple comparisons) (**A**). Gene map showing rs1145887 is an intronic SNP that occurs in a region with acetylated histone H3 marks (H3K27Ac) and within a Dnase I hypersensitivity domain, typical of a regulatory element (**B**). Human pulmonary artery endothelial cells treated with CD70 siRNA demonstrated reduced wound recovery after scratch compared with control cells (**C** and **D**). ***$P<0.001$.

CD70 knockdown significantly reduced maximal agonist-stimulated real-time generation of NO by 26% in HAECs (Figure 2A and 2C) and by 38% in HPAECs (Figure 2B and 2G).

As eNOS is the primary source of NO in endothelial cells, we next evaluated eNOS expression. CD70 knockdown resulted in significant reductions in eNOS protein, with approximately a 50% reduction in eNOS protein levels in HAECs and HPAECs (Figure 2D and H; Figure S2A and S2B). Time-course study of eNOS protein expression showed that protein levels remained low for 3 to 4 days after CD70-targeted

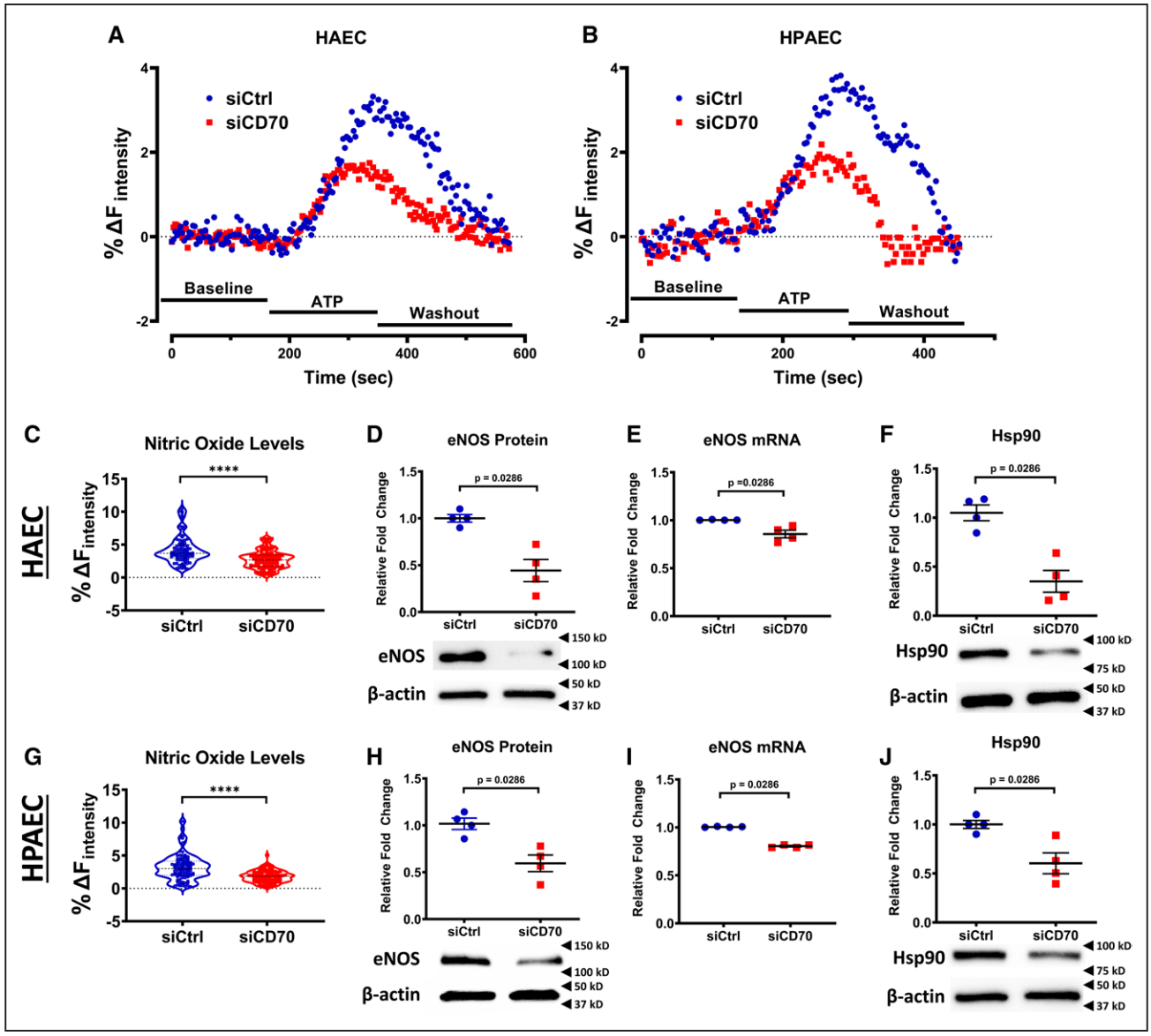

Figure 2. CD70 knockdown reduced cellular NO levels and eNOS (endothelial nitric oxide synthase) expression.
Real-time intracellular levels of NO in human aortic endothelial cells (HAECs) and human pulmonary artery endothelial cells (HPAECs) were measured following stimulation with 30 μM ATP. **A** and **B**, Show representative averaged time curves for baseline fluorescence, ATP treatment, and washout, with greater fluorescence change (%$\Delta F_{intensity}$) correlating with greater NO levels. NO levels were reduced following siRNA-mediated CD70 (siCD70) knockdown compared with control-siRNA-treated cells (siCtrl) for HAECs and HPAECs (**C** and **G**). For HAECs, data represent the median of 89 cells for siCtrl and 129 cells for siCD70, collected over 3 independent experiments. For HPAECs, data represent the median of 105 cells for siCtrl and 106 cells for siCD70 collected over 4 independent experiments. Protein levels (**D** and **H**) mRNA (**E** and **I**) for eNOS were decreased after treatment with siCD70 compared with siCtrl. Protein expression of the eNOS chaperone Hsp90 (heat shock protein 90) was reduced with siCD70 treatment in HAECs and HPAECs (**F** and **J**). For eNOS and Hsp90, representative Western blots are shown along with corresponding densitometry, with values normalized to β-actin levels and expressed as fold change compared with siCtrl. For eNOS mRNA, data are normalized to β-actin mRNA and expressed as fold change compared with siCtrl. Data presented as mean±SE. ****$P<0.0001$.

siRNA transfection (Figure S2C). Quantitative PCR analysis of eNOS transcript levels showed a modest but significant decrease in eNOS mRNA in HAECs and HPAECs after CD70 knockdown (Figure 2E and 2I). Agonist-stimulated NO levels were inhibited with pretreatment of the NOS inhibitor L-N^G-nitro arginine methyl ester, confirming specificity of the signal to NOS (Figure S2J and S2K). Taken together, these data suggest that loss of CD70 inhibits NO production, at least in part, through impaired eNOS expression and reduced eNOS protein levels. NO generation by eNOS is tightly regulated by changes in intracellular calcium. Real-time ratiometric fluorescence imaging using the calcium sensor Fura-2/AM showed that there were no changes in calcium flux in HAECs following stimulation with ATP (Figure S2D); in contrast, CD70-knockdown

HPAECs demonstrated reduced total calcium flux in response to agonist stimulation (Figure S2G).

Endothelial NOS protein function is influenced by several protein-protein interactions. Among these, the interaction of eNOS with the chaperone Hsp90 is important for enzyme activation and stability. In response to CD70 knockdown, we observed that Hsp90 protein levels are decreased in HAECs and HPAECs (Figure 2F and 2J), suggesting a potential role for CD70 in facilitating eNOS-protein interactions. By comparison, expression of caveolin-1, another known eNOS protein partner, was unchanged following CD70 knockdown (Figure S2E, S2F, S2H, S2I). Since eNOS dysregulation and Hsp90 downregulation can be associated with eNOS uncoupling and peroxynitrite formation,[42,43] we sought to determine if CD70 knockdown enhances 3-nitrotyrosine (3-NT) levels as a surrogate for peroxynitrite. By Western blot, we detected 2 major molecular weight species containing 3-NT in HAECs and HPAECs (Figure 3A); levels of both of these species increased following siRNA-mediated CD70 knockdown (Figure 3B through 3E). We next sought to determine if increased superoxide levels may be mediating this increase in protein nitration. Utilizing DHE, we observed an increase in baseline fluorescence in CD70 knockdown cells compared with control cells at the excitation/emission spectrum expected for the superoxide-mediated product 2-hydroxyethidium (Figure 3H). To provide greater specificity that this was reflective of increased superoxide, we stimulated cells with menadione and observed a larger increase in menadione-mediated fluorescence in CD70-knockdown cells; additionally, there was a greater increase in SOD-mediated inhibition of this fluorescence in the CD70-knockdown cells compared with control cells (Figure 3I). Taken together, these data provide evidence for increased superoxide levels in CD70-deficient cells. We concomitantly observed that total nitrite/nitrate levels were similar in control versus CD70-knockdown ECs (Figure 3J), suggesting that NO was being shunted towards peroxynitrite, leading to enhanced 3-NT, before further metabolism to contribute to the overall cellular nitrite/nitrate pool.

With the reduction in NO generation and enhanced 3-NT levels, we next determined the net effect of these changes on NO bioactivity. We assessed intracellular cGMP levels in response to stimulation with ATP and found that these were reduced following CD70 knockdown (Figure 3F and 3G), confirming that NO bioactivity is impaired. These data support the notion that reduced CD70 expression impairs the NO signaling axis by mediating a reduction in eNOS protein expression and downstream NO bioavailability and bioactivity, likely through a reduction in the key protein chaperone Hsp90, and with contributions from elevated ROS levels.

Loss of CD70 Is Associated With Increased Intracellular and Membrane-Associated Hydrogen Peroxide

Redox homeostasis is integral to maintaining normal endothelial function, with redox dysregulation being closely linked to perturbations in eNOS.[44] Given our observations of reduced eNOS protein levels along with decreased NO bioactivity and evidence of increased superoxide levels, we sought to directly assess H_2O_2, a more stable ROS intermediate, using the genetically encoded biosensor Hyper7.2. The Hyper7.2 probe has been extensively characterized to have high specificity and selectivity for detecting intracellular H_2O_2 down to the low nanomolar range.[38,45] HAECs and HPAECs treated with siRNA were transfected with a plasmid for cytosolic expression of Hyper7.2. Auranofin, a well-characterized ROS enhancer that inhibits thiol-reductases including thioredoxin reductases, was utilized as an initiator of oxidative stress. After a 15-minute treatment with auranofin, cells lacking CD70 exhibited faster accumulation of H_2O_2 compared with control cells, with a stronger phenotype seen in HPAECs (Figure 4A and 4B) than HAECs (Figure S3A and S3B). To confirm the specificity of these findings to H_2O_2 generation, pretreatment of cells with catalase abolished the auranofin-induced increase (data not shown).

To define better the nature of ROS augmentation, we sought to determine whether there is specific subcellular localization of the H_2O_2 signal within cells. A major site of cellular ROS generation is the plasma membrane, and within this structure, specialized regions can contain a greater concentration of redox-active enzymes. Caveolar proteins can define lipid rafts and membrane structures that are particularly redox-active,[46,47] and given our results demonstrating eNOS dysregulation, we were interested in the local ROS milieu around the plasma membrane in general and in caveolar structures in particular. We utilized a caveolin-1-directed Hyper7.2 probe for precisely targeted spatial measurements of H_2O_2 levels; given the more prominent HPAEC phenotype, we utilized this cell type for the spatial-targeting studies. With the caveolin-directed Hyper7.2 probe, we observed that H_2O_2 levels over time increased in response to auranofin in CD70-knockdown cells around the caveolin-containing regions of the plasma membrane by up to 60% compared with control cells (Figure 4C and 4D). This subcellular increase in H_2O_2 raised the possibility that membrane-associated ROS generators could be playing a role in the augmented H_2O_2 levels after CD70 knockdown. We also examined H_2O_2 levels after CD70 knockdown in response to a distinct agonist, histamine. Here, again, we observed an increase in cytosolic and caveolar H_2O_2 in HPAECs (Figure 4E and 4F). Taken together, these data suggest a greater propensity for accumulation of intracellular ROS in the setting of reduced expression of CD70 in endothelial cells.

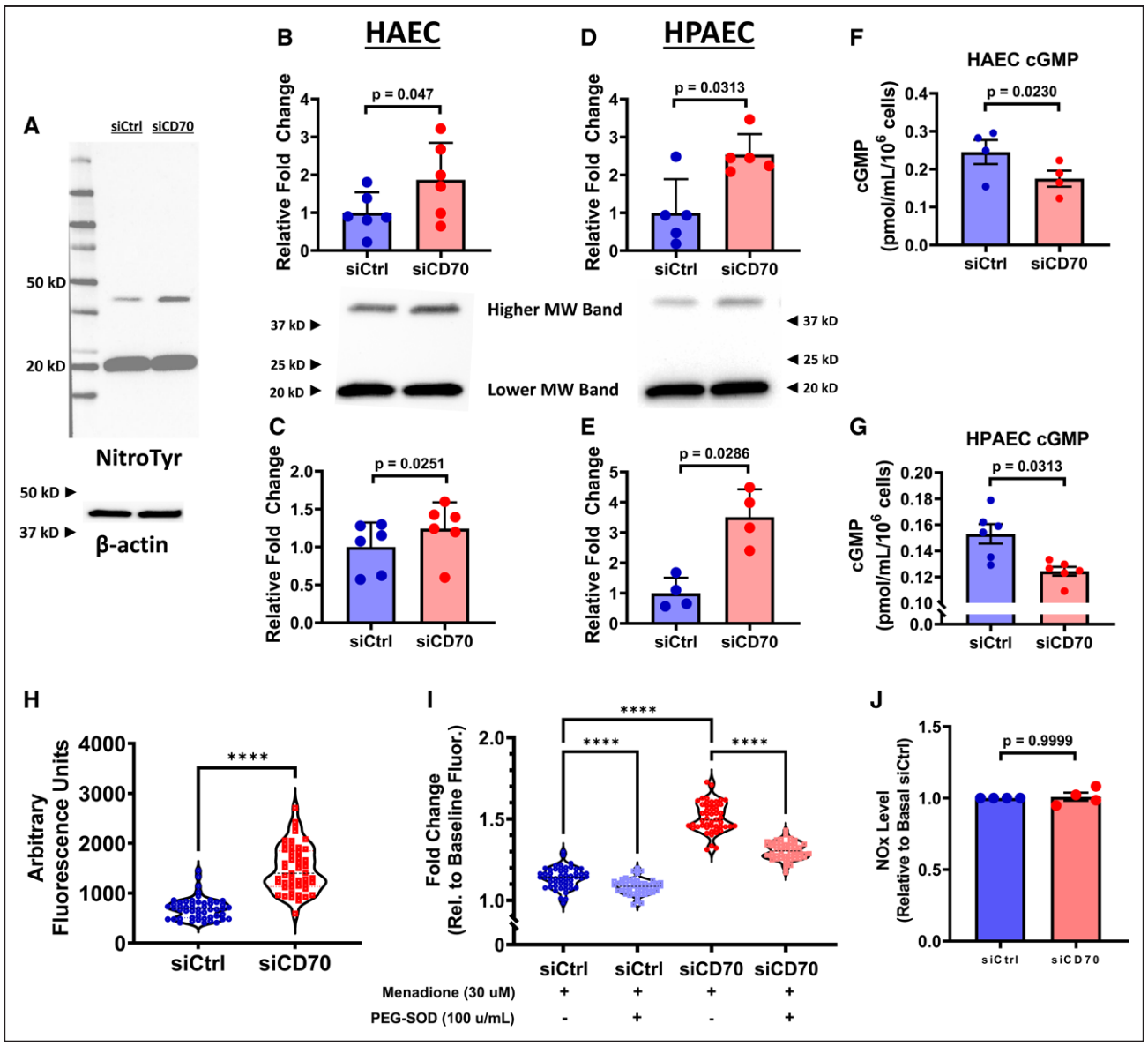

Figure 3. 3-Nitrotyrosine and cellular superoxide are increased and cGMP levels are decreased after CD70 knockdown. Human aortic endothelial cells (HAECs) and human pulmonary artery endothelial cells (HPAECs) were treated with control (siCtrl) vs CD70-directed siRNA (siCD70). Immunoblotting for 3-nitrotyrosine adducts revealed two major species in endothelial cells: a higher molecular weight band corresponding to ≈ 45 kD and a lower molecular weight band corresponding to ≈ 20 kD (**A**). Both bands were increased in siCD70 cells as compared with siCtrl in HAECs (**B** and **C**) and HPAECs (**D** and **E**). Total intracellular cGMP levels were likewise decreased in siCD70 cells compared with siCtrl (**F** and **G**). CD70-knockdown HPAECs loaded with dihydroethidium (DHE) demonstrated increased basal fluorescence in the expected spectrum (excitation 488 nm, emission 588 nm) for 2-hydroethidium, the product of superoxide's reaction with DHE (**H**). Cells loaded with DHE and then subsequently stimulated with menadione showed increased fluorescence in the setting of CD70 knockdown; furthermore, the reduction in fluorescence with PEG-SOD (pegylated superoxide dismutase) was greater in these cells compared with control cells, supporting the specificity of this increased fluorescence to enhanced superoxide levels. Nitrite/nitrate levels are unchanged in control vs CD70-knockdown cells (**J**). For 3-nitrotyrosine, representative Western blots are shown along with corresponding densitometry, with values normalized to β-actin levels and expressed as fold change compared with siCtrl. Data presented as mean±SE. ****P<0.0001.

NOXs are known membrane-associated sources of ROS in ECs that can sub-localize to caveolae-containing regions of the plasma membrane.[48] We, therefore, evaluated expression of NOX1 and NOX2 complexes in response to CD70 knockdown. We found that both NOX1 expression as well as mRNA expression of the NOX1-activating factor NOXA1 were increased in HPAECs (Figure 5A through 5C); similarly, there was an increase in expression of the catalytic subunit of NOX2, gp91phox (Figure 5D and 5E). By comparison, HAECs showed a 2-fold increase in NOXA1 transcript and no change in NOX1 or gp91phox expression (Figure S3C through S3G). These variations in expression of NOXs by cell type reflected the differences in H_2O_2 levels between HAECs and HPAECs noted through our biosensor studies. The key NOX1/NOX2 co-factors p22phox, RAC1,

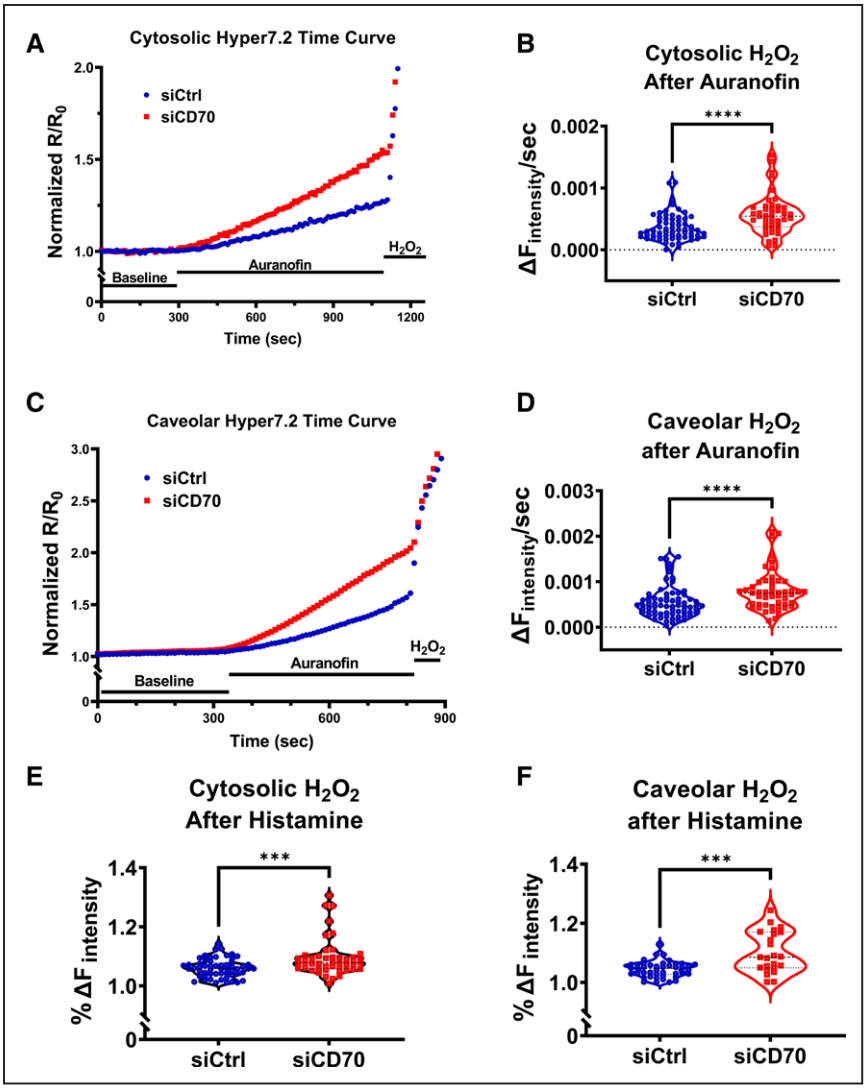

Figure 4. Reduced CD70 expression leads to increased cytosolic and caveolar hydrogen peroxide levels in endothelial cells.
Human pulmonary artery endothelial cells (HPAECs) were treated with control (siCtrl) vs CD70-directed siRNA (siCD70) and subsequently transfected with the genetically encoded biosensor Hyper7.2 for real-time intracellular monitoring of hydrogen peroxide (H_2O_2) in the cytosol (**A**, **B**, and **E**) and plasmalemmal caveolae (**C**, **D**, and **F**). Hydrogen peroxide was assessed by the ratio of fluorescence emission following excitation at 490 nm and 420 nm normalized to baseline fluorescence (normalized R/R_0). Following treatment with 1 μM auranofin, cells were treated with 25 μM H_2O_2 as a positive control. The rate of rise of intracellular H_2O_2, calculated as the slope of the linear portion of the auranofin-treatment curve over the final 300 seconds of drug treatment ($\Delta F_{intensity}$/s), was greater in siCD70-treated cells compared with control cells for both cytosolic (**A** and **B**) and caveolar H_2O_2 (**C** and **D**). Treatment with histamine similarly led to greater cytosolic (**E**) and caveolar H_2O_2 (**F**) levels in CD70-knockdown cells compared with control. All panels were analyzed by unpaired Mann-Whitney *U* test. ***$P<0.001$, ****$P<0.0001$.

and NOXO1, as well as NOX4, showed no difference in expression levels between control and CD70-knockdown cells (Figure S4).

Knockdown of CD70 Alters Antioxidant Enzyme Expression

The enhanced accumulation of endothelial ROS in the setting of CD70 knockdown raised the question of whether loss of CD70 was additionally inducing alterations in antioxidant enzymes, thereby influencing the ROS generation-metabolism equilibrium. To explore this issue, we examined expression of antioxidant enzymes after treatment with CD70-directed siRNA. Given the elevations in NOX1 and gp91phox, we first evaluated copper/zinc superoxide dismutase (SOD1), the major cytosolic enzyme that reduces superoxide to H_2O_2, and found that both transcript and protein levels were elevated (Figure 6A, 6B, 6H, 6I). This increase was associated with a reduction in catalase protein expression by nearly 50% in CD70-knockdown cells (Figure 6C and 6J); catalase mRNA levels were unchanged (Figure S5A and S5D). In comparison, the antioxidant enzyme glutathione peroxidase 1 (GPx-1) demonstrated increased transcript and protein expression (Figure 6D, 6E, 6K, 6L). In addition, GPx activity was increased following treatment with CD70 siRNA (Figure 6F, 6M). Both SOD1 and GPx-1 are regulatory targets of the transcription factor Nrf2 (nuclear factor-erythroid factor 2-related factor 2)/antioxidant response element signaling axis. We sought to determine if expression of Nrf2 was enhanced as a possible mechanism by which to explain our findings about SOD1 and GPx-1. Quantitative RT-PCR demonstrated increased Nrf2 mRNA levels following CD70 knockdown (Figure 6G, 6N), suggesting that the enhanced expression of SOD1 and GPx-1 may involve Nrf2 signaling.

CD70 Knockdown Leads to Elevated Mitochondrial Hydrogen Peroxide

Mitochondria are a major source of ROS in endothelial cells,[49] and we, therefore, sought to determine if CD70

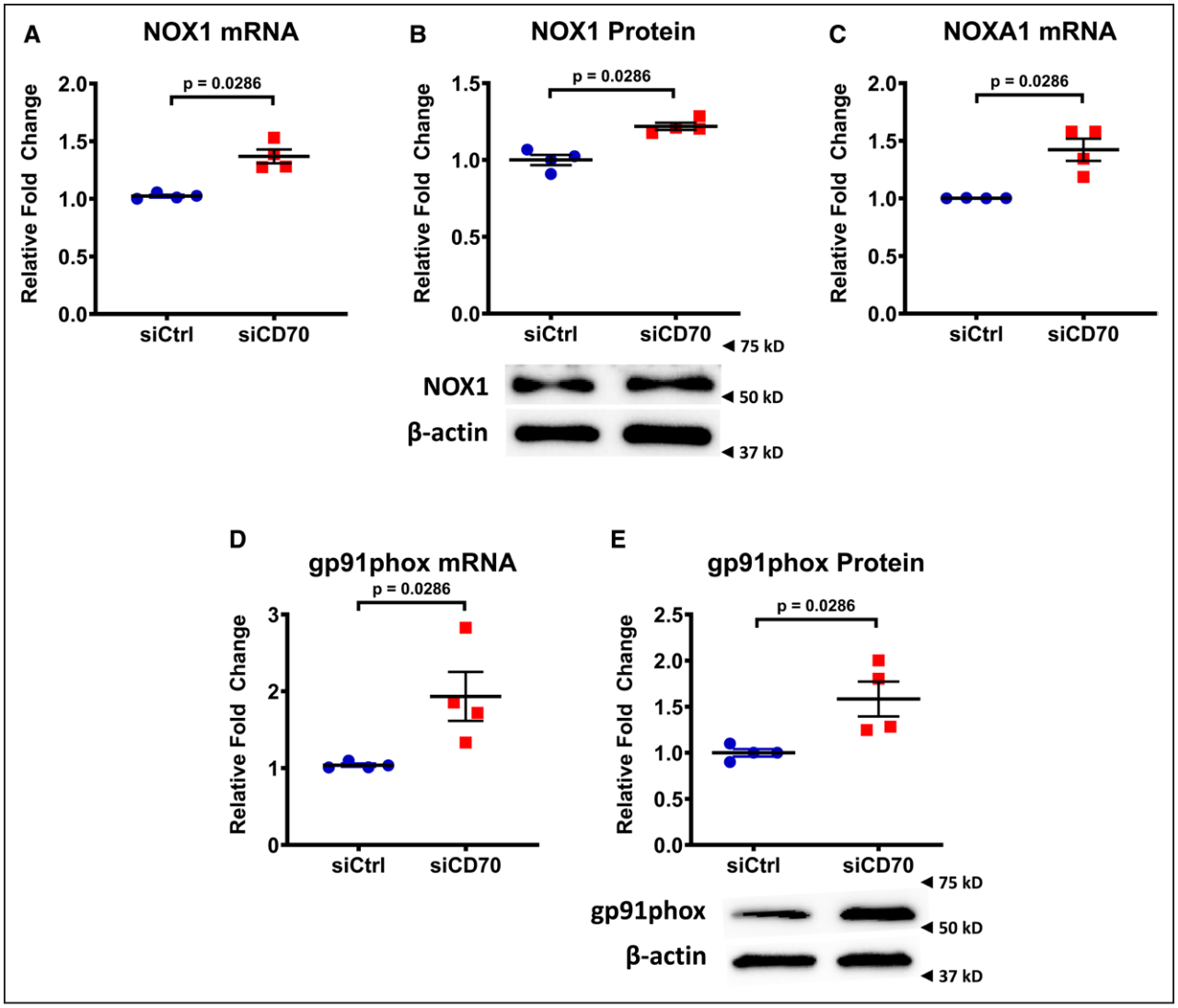

Figure 5. CD70 knockdown is associated with enhanced NOX (NADPH oxidase) expression.
Following CD70 knockdown (siCD70), human pulmonary artery endothelial cells (HPAECs) demonstrated increased NOX (NADPH oxidase) 1 transcript (**A**) and protein (**B**) expression, and NOXA1 mRNA (**C**). Transcript levels of gp91phox, the catalytic subunit of NOX2, were enhanced (**D**), along with the corresponding protein levels of gp91phox (**E**). For NOX1 and gp91phox protein levels, representative Western blots are shown along with corresponding densitometry, with values normalized to β-actin levels and expressed as fold change compared with siCtrl. For NOX1 and NOXA1, mRNA levels are normalized to β-actin mRNA, and for gp91phox, mRNA levels are normalized to RNA polymerase II subunit A mRNA; data are expressed as fold change compared with siCtrl. Data presented as mean±SE.

may affect mitochondrial ROS levels. We utilized a mitochondrial matrix-targeted form of the Hyper7.2 probe to determine H_2O_2 levels in this subcellular compartment following treatment with auranofin. Complementing our findings in the cytosol and around the plasma membrane, here again, we found that mitochondrial H_2O_2 levels increased more rapidly following auranofin treatment in the setting of CD70 knockdown as compared with control cells (Figure 7A and 7B). The enzyme manganese superoxide dismutase (SOD2) has a central role in ROS metabolism within the mitochondrial matrix. To determine if enhanced SOD2 levels could be contributing to our preceding observation, we examined expression of SOD2 following treatment with CD70-directed siRNA. We found that SOD2 abundance is increased, with elevations in both transcript and protein levels, in CD70 knockdown cells compared with control (Figure 7C through 7F). These data provide evidence that ROS levels in the mitochondrial compartment are increased following loss of CD70 expression and mirror the changes in ROS observed in the cytosol and around caveolae.

CD70 Overexpression Enhances NO Levels and Attenuates TNFα-induced eNOS Downregulation

Our data demonstrating the effects of CD70 knockdown raised the question of how CD70 overexpression may affect endothelial cell function. We utilized a plasmid overexpressing CD70 linked to an mCherry reporter;

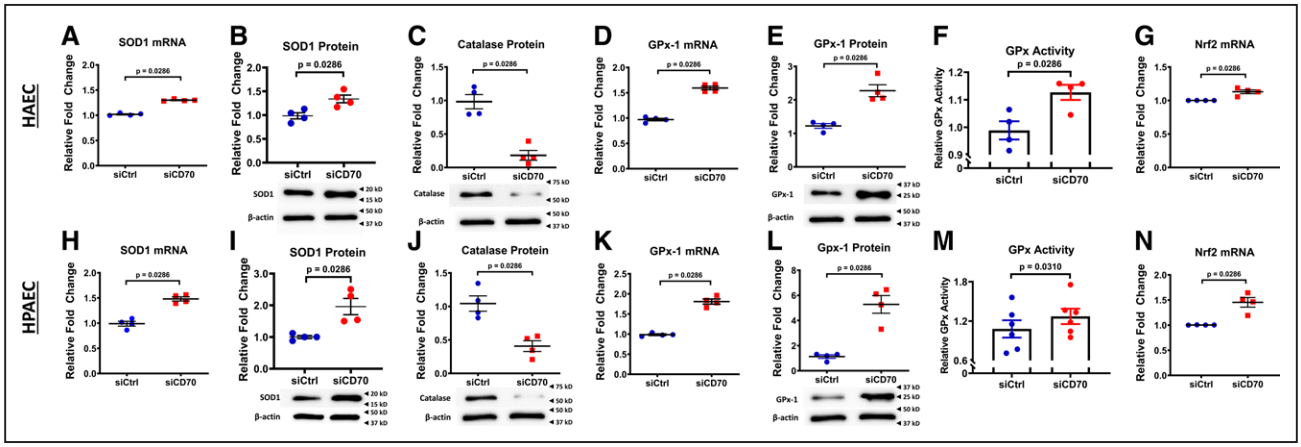

Figure 6. Reduction in CD70 alters endothelial anti-oxidant enzyme expression.
In comparison to control-treated cells (siCtrl), CD70-knockdown cells (siCD70) showed enhanced SOD1 (superoxide dismutase 1) mRNA (**A** and **H**) and protein (**B** and **I**) levels in both human aortic endothelial cells (HAECs) and human pulmonary artery endothelial cells (HPAECs). Catalase protein expression was reduced in siCD70 samples (**C** and **J**); conversely, GPx-1 (glutathione peroxidase 1) mRNA (**D** and **K**) and protein levels (**E** and **L**) were elevated. Total intracellular GPx activity was augmented after treatment with siCD70 (**F** and **M**). Nrf2 (nuclear factor-erythroid factor 2-related factor 2) transcript levels were elevated in siCD70-treated cells (**G** and **N**). For SOD1, catalase and GPx-1 protein levels, representative Western blots are shown along with corresponding densitometry, with values normalized to β-actin levels and expressed as fold change compared with siCtrl. For SOD1, GPx-1, and Nrf2 mRNA levels, data are normalized to β-actin mRNA and expressed as fold change compared with siCtrl. Data presented as mean±SE.

we included a linked reporter due to known issues with antibody-based CD70 protein detection, including band specificity on Western blots.[50–53] HPAECs transfected with this plasmid demonstrated robustly increased expression of CD70 mRNA and protein compared with control-transfected cells (Figure S6A through S6C). To determine what impact this may have on endothelial phenotype, we performed a scratch assay and observed significantly increased wound closure in CD70-overexpressing cells compared with control cells (Figure S6D). This finding was associated with an increase in agonist-stimulated NO levels in the CD70 overexpressing cells and an increase in eNOS mRNA expression (Figure S6E and S6F). We have observed that pathological stimuli, which reduce eNOS expression, including TNFα and glucose deprivation, are associated with elevated CD70 expression (Figure S1A through S1D). Given our observations on the link between CD70 and eNOS, we hypothesized that CD70 upregulation may be serving a counter-regulatory role in the setting of these pathological stimuli. To test this hypothesis, we evaluated the effect of CD70 overexpression on eNOS expression in the setting of TNFα treatment. Compared with control cells, TNFα treatment of cells overexpressing CD70 demonstrated an attenuated reduction in eNOS mRNA levels, partly rescuing this phenotype (Figure S6F).

DISCUSSION

To date, CD70 has primarily been studied in the context of immunobiology and cancer immunotherapy. Our key novel finding is that CD70 plays a previously unrecognized role in endothelial cell biology (Figure 8). Knockdown of CD70 leads to a decrease in eNOS expression and function, as exhibited by reduced NO levels and bioactivity, and impaired endothelial wound closure. Inhibiting CD70 expression also leads to elevated ROS levels and is characterized by upregulation of NOX complex proteins, likely leading to an increase in cellular superoxide. Increased SOD1 expression contributes to cytosolic and caveolar H_2O_2 levels, and increased SOD2 contributes to augmented mitochondrial H_2O_2. Intriguingly, CD70 overexpression is characterized by enhanced eNOS expression and agonist-stimulated NO levels, as well as attenuated downregulation of eNOS mRNA in response to TNFα. Finally, SNPs in CD70 associate with human vascular disease phenotypes in a phenome-wide analysis, demonstrating the clinical relevance of CD70 in vascular pathology.

Our results demonstrate a key intersection between eNOS, a critical determinant of endothelial function, and CD70. Other TNFSF ligands can also regulate eNOS expression and function. TNFα can downregulate eNOS by promoting eNOS mRNA instability,[54–56] and treatment with sCD40L has been shown to reduce NO and eNOS protein levels in vitro and ex vivo.[57,58] In both cases, increased exposure to the TNFSF ligand leads to reduced eNOS levels and decreased enzyme activity. Our findings suggest a role for CD70 that is opposite in directionality to these other TNFSFs. Loss of CD70 leads to reduced eNOS expression and agonist-stimulated NO, while CD70 overexpression leads to enhanced eNOS mRNA expression and NO levels. This difference in effect suggests complex and counter-regulatory pathways involving TNFSFs in endothelial cells. Since expression of many TNFSFs can be induced by

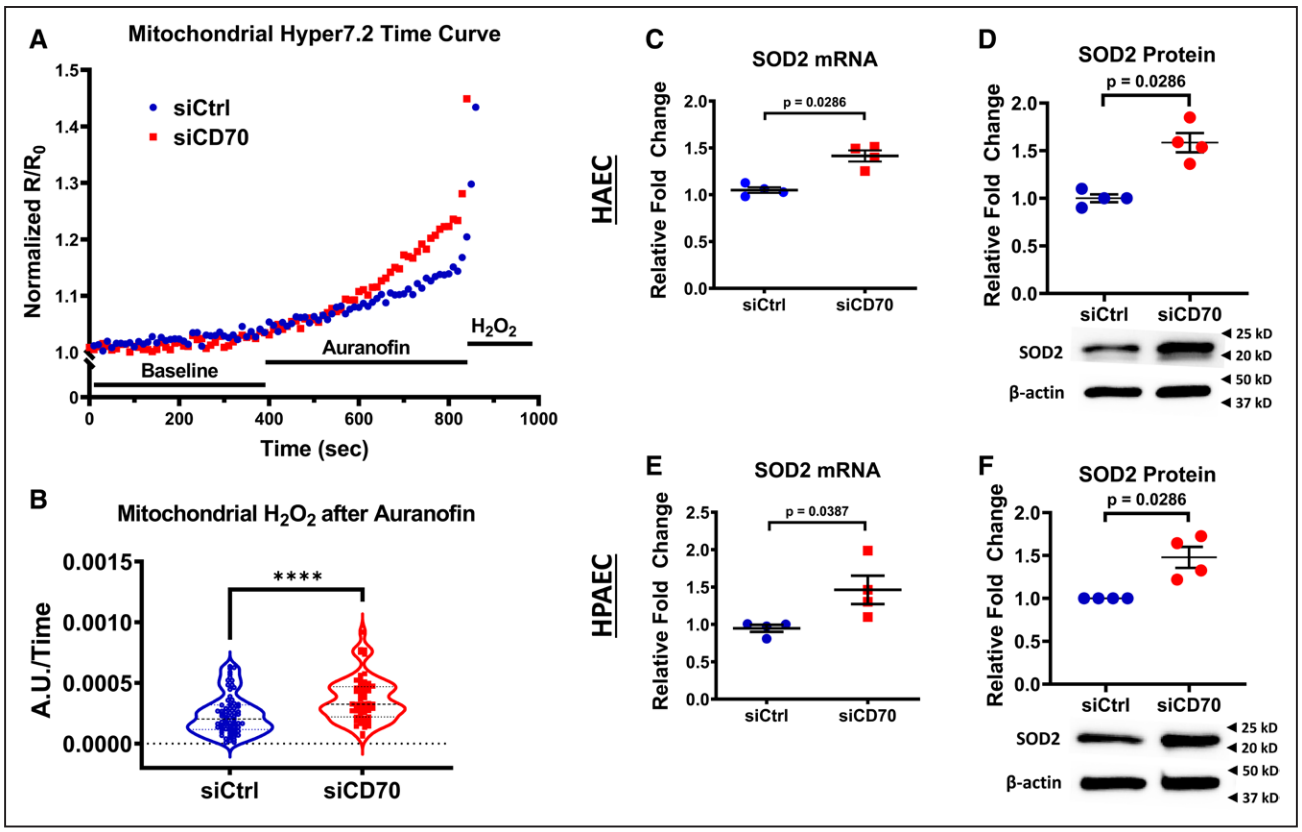

Figure 7. CD70 knockdown leads to increased mitochondrial hydrogen peroxide levels.
Following treatment with CD70 siRNA, human pulmonary artery endothelial cells (HPAECs) showed faster accumulation of hydrogen peroxide in the mitochondrial matrix in response to treatment with 1 mmol/L auranofin (**A** and **B**). SOD2 transcript (**C** and **E**) and protein (**D** and **F**) expression were correspondingly increased after CD70 knockdown compared with control cells in human aortic endothelial cells (HAECs) and HPAECs. Representative Western blots are shown for SOD2 along with corresponding densitometry, with values normalized to β-actin levels and expressed as fold change compared with siCtrl. For SOD2 mRNA, data are normalized to β-actin mRNA and expressed as fold change compared with siCtrl. Data presented as mean±SE. ****P<0.0001.

common inflammatory mediators,[39,59] a single activating signal may mobilize competing TNFSF pathways to both propagate and counteract this signal, suggesting a role for TNFSFs broadly, and CD70 in particular, in the maintenance of endothelial homeostasis. Our data provide support for the notion that CD70 may serve such a homeostatic role to oppose the effects of stimuli such as TNFα and, thereby, help maintain eNOS expression and NO levels. TNFSFs demonstrate this counterbalancing effect in other contexts, such as opposing effects on cell proliferation versus apoptosis: TNF-α and receptor activator of nuclear factor-κB ligand can promote proliferative signals while CD95 and TNF-related apoptosis-inducing ligand (TRAIL) oppose this effect.[60]

An understanding of the role of CD70 in the control of vascular function is rudimentary. Descriptive histological analyses have identified expression of CD70 in vascular tissue,[19,24] although the functional effects of this expression have not been examined previously. In one study by Simons et al,[25] CD70$^{-/-}$ mice exhibited impaired collateral vessel formation and decreased CD31^{+} endothelial cells in muscle samples following hindlimb ischemia. Our results support this impact of CD70 on endothelial growth and function and provide a mechanistic basis for these findings that centers on NO. Loss of CD70 leads to reduced levels of eNOS with a resulting decrease in both agonist-stimulated NO generation and NO bioactivity. This provides a plausible explanation for the observed impact that loss of CD70 has on angiogenesis and vascular homeostasis.

Expression and function of the eNOS protein is tightly regulated through several mechanisms, including post-transcriptional, post-translational, and protein-protein effects. Our findings indicate that one such critical regulator that is affected by loss of CD70 is Hsp90, one of the key protein binding partners for eNOS. Formation of a heterocomplex between eNOS and Hsp90 can facilitate heme insertion into the enzyme, promote conformational activation of eNOS, and facilitate Akt-mediated eNOS phosphorylation.[61,62] Loss of the eNOS-Hsp90 interaction has been shown to affect eNOS protein levels, in part, due to increased eNOS degradation by the ubiquitin-proteasome system and the cysteine protease calpain.[63–67] In an analogous manner, our data suggest that the reduction in eNOS protein observed with knockdown of CD70 may be, in

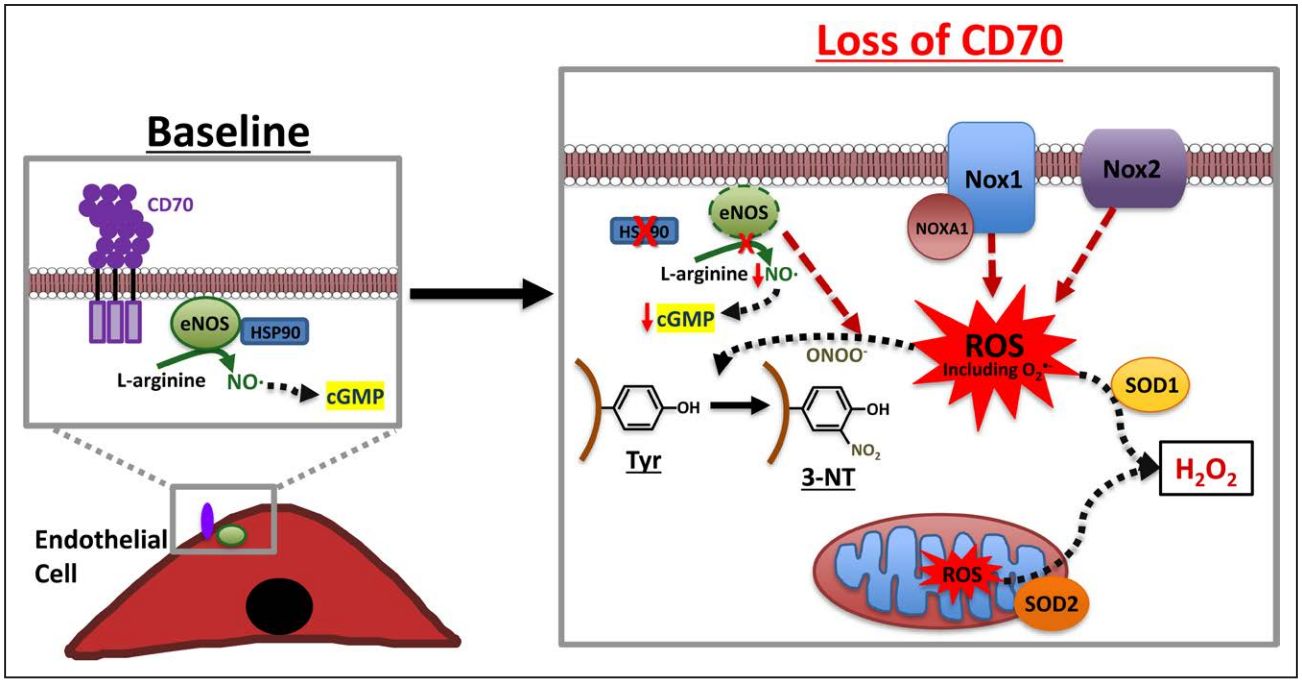

Figure 8. Working model for changes in endothelial cell signaling induced by CD70 ablation.
Loss of CD70 leads to reduced eNOS (endothelial nitric oxide synthase) protein and decreased NO levels with concomitant increase in intracellular reactive oxygen species from several sources.

part, due to enhanced eNOS susceptibility to degradation secondary to a reduction in Hsp90 protein levels. Other TNFSF ligands have also been shown to regulate HSP90. In a cancer cell line, treatment with TNF-α and TRAIL induced cleavage of HSP90 and resulted in cellular apoptosis, suggesting crosstalk between TNFSFs and this intracellular chaperone.[68]

We observed increased H_2O_2 levels in response to downregulation of CD70. Hydrogen peroxide is a stable ROS intermediate that can also function as a signaling molecule within and between vascular cells[69]; assessment of H_2O_2 levels, thus, provides not only an important marker for ROS status but also can suggest functional consequences within endothelial cells. Our results with auranofin, a well-characterized enhancer of ROS that is utilized in patients as a treatment for rheumatoid arthritis, provide support that CD70 knockdown creates a pro-oxidant environment within multiple cellular compartments. It is important to note that our results showing enhanced H_2O_2 levels in response to an endogenous mediator, histamine, in addition to an exogenous pharmacological agent, strongly suggest that the auranofin results are not simply a reflection of drug treatment or alterations in biosensor redox cycling; histamine-mediated effects would reflect a distinct pathway for H_2O_2 generation involving receptor activation and intracellular calcium release.[70]

There are several potential sources of ROS that may be contributing to the enhanced intracellular levels of H_2O_2 in response to CD70 knockdown. We identified that cytosolic, caveolar, and mitochondrial H_2O_2 levels are all increased. Our findings of increased NOX1 and NOX2 expression along with enhanced SOD1 levels provide one possible mechanism for the augmented cytosolic and plasma-membrane-associated H_2O_2 increases. NOXs are a major source of ROS generation in endothelial cells. Endothelial cells express a variety of NOX complexes, including NOX1 and NOX2, which are the primary inducible forms, as well as NOX4, which is the most highly expressed isoform.[71] ROS produced from NOX1 and NOX2 can potentiate endothelial dysfunction,[72–75] and NOXs have been shown to cluster around caveolin-containing lipid rafts in the endothelial cell membranes.[48,76] Other TNFSF ligands have been shown to affect NOX expression. Stimulation of coronary artery endothelial cells with TNF-α and Fas ligand can induce clustering of lipid rafts containing gp91phox and stimulate clustering with the NOX2 cofactors p47phox and RAC1.[77] Treatment of coronary artery endothelial cells with sCD40L can increase NOX activity, likely involving NOX4.[58] TNF-α is well known to augment endothelial ROS levels through both mitochondrial sources and NOXs.[78]

The enhanced mitochondrial levels of H_2O_2 also raise the possibility that loss of CD70 may be inducing alterations in mitochondrial function and endothelial metabolism. Inflammatory signals have been shown to influence endothelial energetics by regulating energy production through glycolysis and oxidative respiration and by altering glucose and fatty acid metabolism.[34,79] Our data demonstrating that a low glucose environment leads to an upregulation of CD70, coupled with alterations observed in cellular ROS after perturbation in CD70 expression,

raise the intriguing possibility that CD70 may be mediating effects through systems that modulate both NO and ROS, including PI3K/Akt and AMP kinase pathways. How CD70 may intersect into these pathways in endothelial cells remains to be determined.

Our observation of altered eNOS function raises the possibility that eNOS uncoupling may be contributing to cellular oxidative stress. It is known that eNOS dysfunction can lead to the enzyme itself becoming a source of ROS through the formation of superoxide and peroxynitrite.[44] Our finding that 3-NT levels were increased along with data supporting elevated superoxide levels in CD70-knockdown cells would provide support for this possible source of ROS. The reaction between NO and superoxide occurs at near diffusion-limited kinetics,[80,81] and, thus, we suspect that in the presence of increased superoxide, NO is preferentially shunted toward peroxynitrite, leading to enhanced protein nitration and elevated 3-NT levels. However, it should be acknowledged that 3-NT can form through other pathways as well, including through the action of myeloperoxidase[82,83] and through the reaction of NO with superoxide from any source, not just uncoupled eNOS.

Our pilot PheWAS analysis suggests a novel association of CD70 with human vascular disease phenotypes. It is worth noting that within the broad grouping of cardiovascular diagnoses, our unbiased PheWAS analysis specifically identified vascular and thrombotic diagnoses rather than myocardial, valvular, or arrhythmic diagnoses. Our results demonstrating a close link between CD70 and eNOS provide a rationale for this observation; CD70 would be expected to associate with conditions in which the endothelium is central to the disease process. Further studies are needed to refine this relationship in larger cohorts of patients, and to identify potential genetic variants that may modify CD70 expression, given the intronic nature of the key SNP. However, the data presented here provide evidence that CD70 may prove to be an attractive target for monitoring of and therapeutic strategies geared towards NO levels and bioactivity in endothelial cells.

ARTICLE INFORMATION

Received February 2, 2022; accepted July 21, 2022.

Affiliations

Division of Cardiovascular Medicine, Department of Medicine, Brigham and Women's Hospital and Harvard Medical School, Boston, MA (A.K.P., M.W.-W., W.X., S.Y., T.M., J.L.). Division of Cardiovascular Medicine, Department of Medicine, Vanderbilt University, Nashville, TN (Q.S.W.). Faculty for Engineering and Natural Sciences, Sabanci University, Istanbul, Turkey (E.E.).

Acknowledgments

The authors thank Stephanie C. Tribuna for expert technical assistance.

Sources of Funding

This work was supported in part by NIH grants HL119145, HL155107, HL155096, and HG007690 to J. Loscalzo; by NIH grants AG63072, HL152173, and HL157918 to T. Michel; and by American Heart Association grants D700382 and CV-19, to J. Loscalzo.

Disclosures

None.

Supplemental Material

Figures S1–S6
Table S1
Major Resources Table
Unedited blots

REFERENCES

1. Deanfield JE, Halcox JP, Rabelink TJ. Endothelial function and dysfunction: testing and clinical relevance. *Circulation*. 2007;115:1285–1295. doi: 10.1161/CIRCULATIONAHA.106.652859
2. Sugamura K, Keaney JF Jr. Reactive oxygen species in cardiovascular disease. *Free Radic Biol Med*. 2011;51:978–992. doi: 10.1016/j.freeradbiomed.2011.05.004
3. Zhang H, Park Y, Wu J, Chen Xp, Lee S, Yang J, Dellsperger KC, Zhang C. Role of TNF-alpha in vascular dysfunction. *Clin Sci (Lond)*. 2009;116:219–230. doi: 10.1042/CS20080196
4. Olofsson PS, Söderström LA, Wågsäter D, Sheikine Y, Ocaya P, Lang F, Rabu C, Chen L, Rudling M, Aukrust P, et al. CD137 is expressed in human atherosclerosis and promotes development of plaque inflammation in hypercholesterolemic mice. *Circulation*. 2008;117:1292–1301. doi: 10.1161/CIRCULATIONAHA.107.699173
5. Wang X, Ria M, Kelmenson PM, Eriksson P, Higgins DC, Samnegård A, Petros C, Rollins J, Bennet AM, Wiman B, et al. Positional identification of TNFSF4, encoding OX40 ligand, as a gene that influences atherosclerosis susceptibility. *Nat Genet*. 2005;37:365–372. doi: 10.1038/ng1524
6. Matsumura Y, Imura A, Hori T, Uchiyama T, Imamura S. Localization of OX40/gp34 in inflammatory skin diseases: a clue to elucidate the interaction between activated T cells and endothelial cells in infiltration. *Arch Dermatol Res*. 1997;289:653–656. doi: 10.1007/s004030050255
7. Kotani A, Hori T, Matsumura Y, Uchiyama T. Signaling of gp34 (OX40 ligand) induces vascular endothelial cells to produce a CC chemokine RANTES/CCL5. *Immunol Lett*. 2002;84:1–7. doi: 10.1016/s0165-2478(02)00082-2
8. Schönbeck U, Libby P. CD40 signaling and plaque instability. *Circ Res*. 2001;89:1092–1103. doi: 10.1161/hh2401.101272
9. Chakrabarti S, Blair P, Freedman JE. CD40-40L signaling in vascular inflammation. *J Biol Chem*. 2007;282:18307–18317. doi: 10.1074/jbc.M700211200
10. Jeon HJ, Choi JH, Jung IH, Park JG, Lee MR, Lee MN, Kim B, Yoo JY, Jeong SJ, Kim DY, et al. CD137 (4-1BB) deficiency reduces atherosclerosis in hyperlipidemic mice. *Circulation*. 2010;121:1124–1133. doi: 10.1161/CIRCULATIONAHA.109.882704
11. Rabieyousefi M, Soroosh P, Satoh K, Date F, Ishii N, Yamashita M, Oka M, McMurtry IF, Shimokawa H, Nose M, et al. Indispensable roles of OX40L-derived signal and epistatic genetic effect in immune-mediated pathogenesis of spontaneous pulmonary hypertension. *BMC Immunol*. 2011;12:67. doi: 10.1186/1471-2172-12-67
12. van Wanrooij EJ, van Puijvelde GH, de Vos P, Yagita H, van Berkel TJ, Kuiper J. Interruption of the Tnfrsf4/Tnfsf4 (OX40/OX40L) pathway attenuates atherogenesis in low-density lipoprotein receptor-deficient mice. *Arterioscler Thromb Vasc Biol*. 2007;27:204–210. doi: 10.1161/01.ATV.0000251007.07648.81
13. Wagner AH, Güldenzoph B, Lienenlüke B, Hecker M. CD154/CD40-mediated expression of CD154 in endothelial cells: consequences for endothelial cell-monocyte interaction. *Arterioscler Thromb Vasc Biol*. 2004;24:715–720. doi: 10.1161/01.ATV.0000122853.99978.b1
14. Imaizumi T, Itaya H, Fujita K, Kudoh D, Kudoh S, Mori K, Fujimoto K, Matsumiya T, Yoshida H, Satoh K. Expression of tumor necrosis factor-alpha in cultured human endothelial cells stimulated with lipopolysaccharide or interleukin-1alpha. *Arterioscler Thromb Vasc Biol*. 2000;20:410–415. doi: 10.1161/01.atv.20.2.410
15. Mach F, Schönbeck U, Sukhova GK, Bourcier T, Bonnefoy JY, Pober JS, Libby P. Functional CD40 ligand is expressed on human vascular endothelial cells, smooth muscle cells, and macrophages: implications for CD40-CD40 ligand signaling in atherosclerosis. *Proc Natl Acad Sci U S A*. 1997;94:1931–1936. doi: 10.1073/pnas.94.5.1931
16. Borst J, Hendriks J, Xiao Y. CD27 and CD70 in T cell and B cell activation. *Curr Opin Immunol*. 2005;17:275–281. doi: 10.1016/j.coi.2005.04.004

17. Itani HA, Xiao L, Saleh MA, Wu J, Pilkinton MA, Dale BL, Barbaro NR, Foss JD, Kirabo A, Montaniel KR, et al. CD70 exacerbates blood pressure elevation and renal damage in response to repeated hypertensive stimuli. *Circ Res*. 2016;118:1233–1243. doi: 10.1161/CIRCRESAHA.115.308111
18. Claus C, Riether C, Schürch C, Matter MS, Hilmenyuk T, Ochsenbein AF. CD27 signaling increases the frequency of regulatory T cells and promotes tumor growth. *Cancer Res*. 2012;72:3664–3676. doi: 10.1158/0008-5472.CAN-11-2791
19. De Meulenaere A, Vermassen T, Aspeslagh S, Zwaenepoel K, Deron P, Duprez F, Ferdinande L, Rottey S. CD70 expression and its correlation with clinicopathological variables in squamous cell carcinoma of the head and neck. *Pathobiology*. 2016;83:327–333. doi: 10.1159/000446569
20. Jacobs J, Deschoolmeester V, Zwaenepoel K, Rolfo C, Silence K, Rottey S, Lardon F, Smits E, Pauwels P. CD70: An emerging target in cancer immunotherapy. *Pharmacol Ther*. 2015;155:1–10. doi: 10.1016/j.pharmthera.2015.07.007
21. Jilaveanu LB, Sznol J, Aziz SA, Duchen D, Kluger HM, Camp RL. CD70 expression patterns in renal cell carcinoma. *Hum Pathol*. 2012;43:1394–1399. doi: 10.1016/j.humpath.2011.10.014
22. Wischhusen J, Jung G, Radovanovic I, Beier C, Steinbach JP, Rimner A, Huang H, Schulz JB, Ohgaki H, Aguzzi A, et al. Identification of CD70-mediated apoptosis of immune effector cells as a novel immune escape pathway of human glioblastoma. *Cancer Res*. 2002;62:2592–2599.
23. Leick MB, Silva H, Scarfò I, Larson R, Choi BD, Bouffard AA, Gallagher K, Schmidts A, Bailey SR, Kann MC, et al. Non-cleavable hinge enhances avidity and expansion of CAR-T cells for acute myeloid leukemia. *Cancer Cell*. 2022;40:494–508.e5. doi: 10.1016/j.ccell.2022.04.001
24. Seko Y, Takahashi N, Tada Y, Yagita H, Okumura K, Nagai R. Restricted usage of t-cell receptor vgamma-vdelta genes and expression of costimulatory molecules in takayasu's arteritis. *Int J Cardiol*. 2000;75 Suppl 1:S77–83; discussion S85–77. doi: 10.1016/s0167-5273(00)00194-7
25. Simons KH, Aref Z, Peters HAB, Welten SP, Nossent AY, Jukema JW, Hamming JF, Arens R, de Vries MR, Quax PHA. The role of CD27-CD70-mediated T cell co-stimulation in vasculogenesis, arteriogenesis and angiogenesis. *Int J Cardiol*. 2018;260:184–190. doi: 10.1016/j.ijcard.2018.02.015
26. Roden DM, Pulley JM, Basford MA, Bernard GR, Clayton EW, Balser JR, Masys DR. Development of a large-scale de-identified DNA biobank to enable personalized medicine. *Clin Pharmacol Ther*. 2008;84:362–369. doi: 10.1038/clpt.2008.89
27. Purcell S, Neale B, Todd-Brown K, Thomas L, Ferreira MA, Bender D, Maller J, Sklar P, de Bakker PI, Daly MJ, et al. PLINK: a tool set for whole-genome association and population-based linkage analyses. *Am J Hum Genet*. 2007;81:559–575. doi: 10.1086/519795
28. Zuvich RL, Armstrong LL, Bielinski SJ, Bradford Y, Carlson CS, Crawford DC, Crenshaw AT, de Andrade M, Doheny KF, Haines JL, et al. Pitfalls of merging GWAS data: lessons learned in the eMERGE network and quality control procedures to maintain high data quality. *Genet Epidemiol*. 2011;35:887–898. doi: 10.1002/gepi.20639
29. Delaneau O, Zagury JF, Marchini J. Improved whole-chromosome phasing for disease and population genetic studies. *Nat Methods*. 2013;10:5–6. doi: 10.1038/nmeth.2307
30. Denny JC, Bastarache L, Ritchie MD, Carroll RJ, Zink R, Mosley JD, Field JR, Pulley JM, Ramirez AH, Bowton E, et al. Systematic comparison of phenome-wide association study of electronic medical record data and genome-wide association study data. *Nat Biotechnol*. 2013;31:1102–1110. doi: 10.1038/nbt.2749
31. Denny JC, Ritchie MD, Basford MA, Pulley JM, Bastarache L, Brown-Gentry K, Wang D, Masys DR, Roden DM, Crawford DC. PheWAS: demonstrating the feasibility of a phenome-wide scan to discover gene-disease associations. *Bioinformatics*. 2010;26:1205–1210. doi: 10.1093/bioinformatics/btq126
32. Kent WJ, Sugnet CW, Furey TS, Roskin KM, Pringle TH, Zahler AM, Haussler D. The human genome browser at UCSC. *Genome Res*. 2002;12:996–1006. doi: 10.1101/gr.229102
33. Rosenbloom KR, Sloan CA, Malladi VS, Dreszer TR, Learned K, Kirkup VM, Wong MC, Maddren M, Fang R, Heitner SG, et al. Encode data in the UCSC Genome Browser: year 5 update. *Nucleic Acids Res*. 2013;41(Database issue):D56–D63. doi: 10.1093/nar/gks1172
34. Lee LY, Oldham WM, He H, Wang R, Mulhern R, Handy DE, Loscalzo J. Interferon-γ impairs human coronary artery endothelial glucose metabolism by tryptophan catabolism and activates fatty acid oxidation. *Circulation*. 2021;144:1612–1628. doi: 10.1161/CIRCULATIONAHA.121.053960
35. Eroglu E, Bischof H, Charoensin S, Waldeck-Weiermaier M, Graier WF, Malli R. Real-time imaging of nitric oxide signals in individual cells using geNOps. *Methods Mol Biol*. 2018;1747:23–34. doi: 10.1007/978-1-4939-7695-9_3
36. Eroglu E, Saravi SSS, Sorrentino A, Steinhorn B, Michel T. Discordance between eNOS phosphorylation and activation revealed by multispectral imaging and chemogenetic methods. *Proc Natl Acad Sci U S A*. 2019;116:20210–20217. doi: 10.1073/pnas.1910942116
37. Eroglu E, Gottschalk B, Charoensin S, Blass S, Bischof H, Rost R, Madreiter-Sokolowski CT, Pelzmann B, Bernhart E, Sattler W, et al. Development of novel FP-based probes for live-cell imaging of nitric oxide dynamics. *Nat Commun*. 2016;7:10623. doi: 10.1038/ncomms10623
38. Pak VV, Ezeriņa D, Lyublinskaya OG, Pedre B, Tyurin-Kuzmin PA, Mishina NM, Thauvin M, Young D, Wahni K, Martínez Gache SA, et al. Ultrasensitive genetically encoded indicator for hydrogen peroxide identifies roles for the oxidant in cell migration and mitochondrial function. *Cell Metab*. 2020;31:642–653.e6. doi: 10.1016/j.cmet.2020.02.003
39. Shiao SL, McNiff JM, Pober JS. Memory T cells and their costimulators in human allograft injury. *J Immunol*. 2005;175:4886–4896. doi: 10.4049/jimmunol.175.8.4886
40. Farah C, Michel LYM, Balligand JL. Nitric oxide signalling in cardiovascular health and disease. *Nat Rev Cardiol*. 2018;15:292–316. doi: 10.1038/nrcardio.2017.224
41. Liu VW, Huang PL. Cardiovascular roles of nitric oxide: a review of insights from nitric oxide synthase gene disrupted mice. *Cardiovasc Res*. 2008;77:19–29. doi: 10.1016/j.cardiores.2007.06.024
42. Sud N, Sharma S, Wiseman DA, Harmon C, Kumar S, Venema RC, Fineman JR, Black SM. Nitric oxide and superoxide generation from endothelial NOS: modulation by HSP90. *Am J Physiol Lung Cell Mol Physiol*. 2007;293:L1444–L1453. doi: 10.1152/ajplung.00175.2007
43. Pritchard KA Jr, Ackerman AW, Gross ER, Stepp DW, Shi Y, Fontana JT, Baker JE, Sessa WC. Heat shock protein 90 mediates the balance of nitric oxide and superoxide anion from endothelial nitric-oxide synthase. *J Biol Chem*. 2001;276:17621–17624. doi: 10.1074/jbc.C100084200
44. Cai H, Harrison DG. Endothelial dysfunction in cardiovascular diseases: the role of oxidant stress. *Circ Res*. 2000;87:840–844. doi: 10.1161/01.res.87.10.840
45. Waldeck-Weiermair M, Yadav S, Spyropoulos F, Krüger C, Pandey AK, Michel T. Dissecting in vivo and in vitro redox responses using chemogenetics. *Free Radic Biol Med*. 2021;177:360–369. doi: 10.1016/j.freeradbiomed.2021.11.006
46. Li PL, Zhang Y, Yi F. Lipid raft redox signaling platforms in endothelial dysfunction. *Antioxid Redox Signal*. 2007;9:1457–1470. doi: 10.1089/ars.2007.1667
47. Patel HH, Insel PA. Lipid rafts and caveolae and their role in compartmentation of redox signaling. *Antioxid Redox Signal*. 2009;11:1357–1372. doi: 10.1089/ars.2008.2365
48. Yang B, Rizzo V. TNF-alpha potentiates protein-tyrosine nitration through activation of NADPH oxidase and eNOS localized in membrane rafts and caveolae of bovine aortic endothelial cells. *Am J Physiol Heart Circ Physiol*. 2007;292:H954–H962. doi: 10.1152/ajpheart.00758.2006
49. Handy DE, Loscalzo J. Redox regulation of mitochondrial function. *Antioxid Redox Signal*. 2012;16:1323–1367. doi: 10.1089/ars.2011.4123
50. Goodwin RG, Alderson MR, Smith CA, Armitage RJ, VandenBos T, Jerzy R, Tough TW, Schoenborn MA, Davis-Smith T, Hennen K. Molecular and biological characterization of a ligand for CD27 defines a new family of cytokines with homology to tumor necrosis factor. *Cell*. 1993;73:447–456. doi: 10.1016/0092-8674(93)90133-b
51. Hintzen RQ, Lens SM, Beckmann MP, Goodwin RG, Lynch D, van Lier RA. Characterization of the human CD27 ligand, a novel member of the TNF gene family. *J Immunol*. 1994;152:1762–1773.
52. Lens SM, Drillenburg P, den Drijver BF, van Schijndel G, Pals ST, van Lier RA, van Oers MH. Aberrant expression and reverse signalling of CD70 on malignant B cells. *Br J Haematol*. 1999;106:491–503. doi: 10.1046/j.1365-2141.1999.01573.x
53. Ryan MC, Kostner H, Gordon KA, Duniho S, Sutherland MK, Yu C, Kim KM, Nesterova A, Anderson M, McEarchern JA, et al. Targeting pancreatic and ovarian carcinomas using the auristatin-based anti-CD70 antibody-drug conjugate SGN-75. *Br J Cancer*. 2010;103:676–684. doi: 10.1038/sj.bjc.6605816
54. Nishida K, Harrison DG, Navas JP, Fisher AA, Dockery SP, Uematsu M, Nerem RM, Alexander RW, Murphy TJ. Molecular cloning and characterization of the constitutive bovine aortic endothelial cell nitric oxide synthase. *J Clin Invest*. 1992;90:2092–2096. doi: 10.1172/JCI116092
55. Marsden PA, Schappert KT, Chen HS, Flowers M, Sundell CL, Wilcox JN, Lamas S, Michel T. Molecular cloning and characterization of human endothelial nitric oxide synthase. *FEBS Lett*. 1992;307:287–293. doi: 10.1016/0014-5793(92)80697-f

56. Yoshizumi M, Perrella MA, Burnett JC Jr, Lee ME. Tumor necrosis factor downregulates an endothelial nitric oxide synthase mRNA by shortening its half-life. *Circ Res*. 1993;73:205–209. doi: 10.1161/01.res.73.1.205
57. Urbich C, Dernbach E, Aicher A, Zeiher AM, Dimmeler S. CD40 ligand inhibits endothelial cell migration by increasing production of endothelial reactive oxygen species. *Circulation*. 2002;106:981–986. doi: 10.1161/01.cir.0000027107.54614.1a
58. Chen C, Chai H, Wang X, Jiang J, Jamaluddin MS, Liao D, Zhang Y, Wang H, Bharadwaj U, Zhang S, et al. Soluble CD40 ligand induces endothelial dysfunction in human and porcine coronary artery endothelial cells. *Blood*. 2008;112:3205–3216. doi: 10.1182/blood-2008-03-143479
59. Schönbeck U, Libby P. The CD40/CD154 receptor/ligand dyad. *Cell Mol Life Sci*. 2001;58:4–43. doi: 10.1007/pl00000776
60. Aggarwal BB. Signalling pathways of the TNF superfamily: a double-edged sword. *Nat Rev Immunol*. 2003;3:745–756. doi: 10.1038/nri1184
61. Billecke SS, Bender AT, Kanelakis KC, Murphy PJ, Lowe ER, Kamada Y, Pratt WB, Osawa Y. hsp90 is required for heme binding and activation of apo-neuronal nitric-oxide synthase: geldanamycin-mediated oxidant generation is unrelated to any action of hsp90. *J Biol Chem*. 2002;277:20504–20509. doi: 10.1074/jbc.M201940200
62. Fontana J, Fulton D, Chen Y, Fairchild TA, McCabe TJ, Fujita N, Tsuruo T, Sessa WC. Domain mapping studies reveal that the M domain of hsp90 serves as a molecular scaffold to regulate Akt-dependent phosphorylation of endothelial nitric oxide synthase and NO release. *Circ Res*. 2002;90:866–873. doi: 10.1161/01.res.0000016837.26733.be
63. Stangl K, Stangl V. The ubiquitin-proteasome pathway and endothelial (dys) function. *Cardiovasc Res*. 2010;85:281–290. doi: 10.1093/cvr/cvp315
64. Jiang J, Cyr D, Babbitt RW, Sessa WC, Patterson C. Chaperone-dependent regulation of endothelial nitric-oxide synthase intracellular trafficking by the co-chaperone/ubiquitin ligase CHIP. *J Biol Chem*. 2003;278:49332–49341. doi: 10.1074/jbc.M304738200
65. Averna M, Stifanese R, De Tullio R, Passalacqua M, Salamino F, Pontremoli S, Melloni E. Functional role of HSP90 complexes with endothelial nitric-oxide synthase (eNOS) and calpain on nitric oxide generation in endothelial cells. *J Biol Chem*. 2008;283:29069–29076. doi: 10.1074/jbc.M803638200
66. Averna M, Stifanese R, De Tullio R, Salamino F, Pontremoli S, Melloni E. In vivo degradation of nitric oxide synthase (NOS) and heat shock protein 90 (HSP90) by calpain is modulated by the formation of a NOS-HSP90 heterocomplex. *FEBS J*. 2008;275:2501–2511. doi: 10.1111/j.1742-4658.2008.06394.x
67. Su Y, Block ER. Role of calpain in hypoxic inhibition of nitric oxide synthase activity in pulmonary endothelial cells. *Am J Physiol Lung Cell Mol Physiol*. 2000;278:L1204–L1212. doi: 10.1152/ajplung.2000.278.6.L1204
68. Fritsch J, Fickers R, Klawitter J, Särchen V, Zingler P, Adam D, Janssen O, Krause E, Schütze S. TNF induced cleavage of HSP90 by cathepsin D potentiates apoptotic cell death. *Oncotarget*. 2016;7:75774–75789. doi: 10.18632/oncotarget.12411
69. Bretón-Romero R, Lamas S. Hydrogen peroxide signaling in vascular endothelial cells. *Redox Biol*. 2014;2:529–534. doi: 10.1016/j.redox.2014.02.005
70. Shimokawa H. Hydrogen peroxide as an endothelium-derived hyperpolarizing factor. *Pflugers Arch*. 2010;459:915–922. doi: 10.1007/s00424-010-0790-8
71. Drummond GR, Sobey CG. Endothelial NADPH oxidases: which NOX to target in vascular disease? *Trends Endocrinol Metab*. 2014;25:452–463. doi: 10.1016/j.tem.2014.06.012
72. Ghouleh IA, Sahoo S, Meijles DN, Amaral JH, de Jesus DS, Sembrat J, Rojas M, Goncharov DA, Goncharova EA, Pagano PJ. Endothelial Nox1 oxidase assembly in human pulmonary arterial hypertension; driver of Gremlin1-mediated proliferation. *Clin Sci (Lond)*. 2017;131:2019–2035. doi: 10.1042/CS20160812
73. de Jesus DS, DeVallance E, Li Y, Falabella M, Guimaraes D, Shiva S, Kaufman BA, Gladwin MT, Pagano PJ. Nox1/Ref-1-mediated activation of CREB promotes Gremlin1-driven endothelial cell proliferation and migration. *Redox Biol*. 2019;22:101138. doi: 10.1016/j.redox.2019.101138
74. Görlach A, Brandes RP, Nguyen K, Amidi M, Dehghani F, Busse R. A gp91phox containing NADPH oxidase selectively expressed in endothelial cells is a major source of oxygen radical generation in the arterial wall. *Circ Res*. 2000;87:26–32. doi: 10.1161/01.res.87.1.26
75. Landmesser U, Dikalov S, Price SR, McCann L, Fukai T, Holland SM, Mitch WE, Harrison DG. Oxidation of tetrahydrobiopterin leads to uncoupling of endothelial cell nitric oxide synthase in hypertension. *J Clin Invest*. 2003;111:1201–1209. doi: 10.1172/JCI14172
76. Nordzieke DE, Medraño-Fernandez I. The plasma membrane: a platform for intra- and intercellular redox signaling. *Antioxidants (Basel)*. 2018;7:E168. doi: 10.3390/antiox7110168
77. Zhang AY, Yi F, Zhang G, Gulbins E, Li PL. Lipid raft clustering and redox signaling platform formation in coronary arterial endothelial cells. *Hypertension*. 2006;47:74–80. doi: 10.1161/10.1161/01.HYP.0000196727.53300.62
78. Chen X, Andresen1 BT, Hill M, Zhang J, Booth F, Zhang C. Role of reactive oxygen species in tumor necrosis factor-alpha induced endothelial dysfunction. *Curr Hypertens Rev*. 2008;4:245–255. doi: 10.2174/157340208786241336
79. Xiao W, Oldham WM, Priolo C, Pandey AK, Loscalzo J. Immunometabolic endothelial phenotypes: integrating inflammation and glucose metabolism. *Circ Res*. 2021;129:9–29. doi: 10.1161/CIRCRESAHA.120.318805
80. Pryor WA, Squadrito GL. The chemistry of peroxynitrite: a product from the reaction of nitric oxide with superoxide. *Am J Physiol*. 1995;268(5 Pt 1):L699–L722. doi: 10.1152/ajplung.1995.268.5.L699
81. Pacher P, Beckman JS, Liaudet L. Nitric oxide and peroxynitrite in health and disease. *Physiol Rev*. 2007;87:315–424. doi: 10.1152/physrev.00029.2006
82. Baldus S, Eiserich JP, Brennan ML, Jackson RM, Alexander CB, Freeman BA. Spatial mapping of pulmonary and vascular nitrotyrosine reveals the pivotal role of myeloperoxidase as a catalyst for tyrosine nitration in inflammatory diseases. *Free Radic Biol Med*. 2002;33:1010. doi: 10.1016/s0891-5849(02)00993-0
83. Gaut JP, Byun J, Tran HD, Lauber WM, Carroll JA, Hotchkiss RS, Belaaouaj A, Heinecke JW. Myeloperoxidase produces nitrating oxidants in vivo. *J Clin Invest*. 2002;109:1311–1319. doi: 10.1172/JCI15021